

1  
2  
3  
4  
5  
6  
7  
8  
9  
10  
11  
12  
13  
14  
15  
16  
17  
18  
19  
20  
21  
22

Article type : Research Article

**Local Shifts in Inflammatory and Resolving Lipid Mediators in Response to Tendon Overuse**

**Running title:** The mediator lipidome of tendon

James F. Markworth<sup>1,2</sup>, Kristoffer B. Sugg<sup>2,3</sup>, Dylan C. Sarver<sup>2,4</sup>, Krishna Rao Maddipati<sup>5</sup>, Susan V. Brooks<sup>1,6</sup>

<sup>1</sup>Department of Molecular & Integrative Physiology, University of Michigan, Ann Arbor, Michigan.

<sup>2</sup>Department of Orthopaedic Surgery, University of Michigan, Ann Arbor, Michigan.

<sup>3</sup>Department of Surgery, University of Michigan, Ann Arbor, Michigan.

<sup>4</sup>Department of Cellular & Molecular Physiology, Johns Hopkins University, Baltimore, Maryland

<sup>5</sup>Department of Pathology, Lipidomics Core Facility, Wayne State University, Detroit, Michigan.

<sup>6</sup>Department of Biomedical Engineering, University of Michigan, Ann Arbor, Michigan.

Susan V. Brooks, PhD  
Christin Carter-Su Collegiate Professor of Physiology  
Professor of Biomedical Engineering

This is the author manuscript accepted for publication and has undergone full peer review but has not been through the copyediting, typesetting, pagination and proofreading process, which may lead to differences between this version and the [Version of Record](#). Please cite this article as [doi: 10.1002/FSB2.21655](https://doi.org/10.1002/FSB2.21655)

This article is protected by copyright. All rights reserved

23 Professor of Molecular & Integrative Physiology

24 University of Michigan

25 2029 BSRB

26 109 Zina Pitcher Pl.

27 Ann Arbor, MI 48109-2002

28 (734) 936-2147

29 [svbrooks@umich.edu](mailto:svbrooks@umich.edu)

30

31 **Nonstandard abbreviations:**

32 PMN – Polymorphonuclear leukocyte/granulocyte

33 MΦ – Macrophage

34 NSAID – Non-steroidal anti-inflammatory drug

35 LC-MS/MS – Liquid chromatography-tandem mass spectrometry

36 HPLC – High Performance Liquid Chromatography

37 MRM – Multiple reaction monitoring

38 LC – Long-chain

39 PUFA – Polyunsaturated fatty acid

40 n-6 – Omega-6

41 n-3 – Omega 3

42 LA – Linoleic acid

43 ARA – Arachidonic acid (20:4n-6)

44 EPA – Eicosapentaenoic acid (20:5n-3)

45 DPA – Docosapentaenoic acid (20:6n-3)

46 DHA – Docosahexaenoic acid (22:6n-3)

47 COX – Cyclooxygenase

48 LOX – Lipoxygenase

49 CYP – Cytochrome p450/epoxygenase

50 PG – Prostaglandin

51 13,14dh-15k – 13,14-dihydro-15-keto

52 TX – Thromboxane

- 53 HHTrE – Hydroxy-heptadecatrienoic acid
- 54 LT – Leukotriene
- 55 SPM – Specialized pro-resolving mediator
- 56 LX – Lipoxin
- 57 Rv – Resolvin
- 58 RvD – D-series resolvin
- 59 RvE – E-series resolvin
- 60 MaR – Maresin
- 61 PD – Protectin
- 62 HOTrE – Hydroxy-octadecatrienoic acid
- 63 Oxo-OTrE – Oxo-octadecatrienoic acid
- 64 HODE – Hydroxy-octadecadienoic acid
- 65 OxoODE – Oxo-octadecadienoic acid
- 66 HETE – Hydroxy-eicosatetraenoic acid
- 67 HEPE – Hydroxy-eicosapentaenoic acid
- 68 HDoHE – Hydroxy-docosahexaenoic Acid
- 69 HDoPE – Hydroxy-docosapentaenoic acid
- 70 EpOME – Epoxy-octadecenoic acid
- 71 DiHOME – Dihydroxy-octadecenoic acid
- 72 EpETrE – Epoxy-eicosatrienoic acid
- 73 DiHETrE – Dihydroxy-eicosatrienoic acid
- 74 EpETE – Epoxy-eicosatetraenoic acid
- 75 DiHETE – Dihydroxy-eicosatetraenoic acid
- 76 EpDPE – Epoxy-docosapentaenoic acid
- 77 ALX/FPR2 – N-formyl peptide receptor 2
- 78 IACUC – Institutional Animal Care and Use Committee
- 79 OCT – Optimal cutting temperature
- 80 IgG – Immunoglobulin G
- 81 IgM – Immunoglobulin M
- 82 WGA – Wheat germ agglutinin
- 83 PBS – Phosphate buffered saline
- 84 OT – Original tendon
- 85 PCA – Principle component analysis

86 RT-qPCR – Real-time quantitative reverse transcription polymerase chain reaction

87 RNA – Ribonucleic acid

88 mRNA – Messenger ribonucleic acid

89 cDNA - complementary DNA

90 ANOVA – Analysis of variance

91 FC – Fold change

92 SEM – Standard error of the mean

93  
94  
95  
96  
97  
98  
99  
100  
101  
102  
103 **Abstract:**

104 Tendon inflammation has been implicated in both adaptive connective tissue remodeling and overuse-  
105 induced tendinopathy. Lipid mediators control both the initiation and resolution of inflammation, but their roles  
106 within tendon are largely unknown. Here we profiled local shifts in intratendinous lipid mediators via liquid  
107 chromatography-tandem mass spectrometry in response to synergist ablation-induced plantaris tendon overuse.  
108 Sixty-four individual lipid mediators were detected in homogenates of plantaris tendons from ambulatory  
109 control rats. This included many bioactive metabolites of the cyclooxygenase (COX), lipoxygenase (LOX), and  
110 epoxygenase (CYP) pathways. Synergist ablation induced a robust inflammatory response at day 3 post-surgery  
111 characterized by epitenon infiltration of polymorphonuclear leukocytes and monocytes/macrophages (MΦ),  
112 heightened expression of inflammation-related genes, and increased intratendinous concentrations of the pro-  
113 inflammatory eicosanoids thromboxane B<sub>2</sub> and prostaglandin E<sub>2</sub>. By day 7, MΦ became the predominant

114 myeloid cell type in tendon and there were further delayed increases in other COX metabolites including  
115 prostaglandins D<sub>2</sub>, F<sub>2α</sub>, and I<sub>2</sub>. Specialized pro-resolving mediators including protectin D1, resolvin D2 and D6,  
116 as well as related pathway markers of D-resolvins (17-hydroxy-docosaehaenoic acid), E-resolvins (18-  
117 hydroxy-eicosapentaenoic acid), and lipoxins (15-hydroxy-eicosatetraenoic acid) were also increased locally in  
118 response to tendon overuse, as were anti-inflammatory fatty acid epoxides of the CYP pathway (e.g. epoxy-  
119 eicosatrienoic acids). Nevertheless, intratendinous prostaglandins remained markedly increased even following  
120 28 days of tendon overuse together with a lingering MΦ presence. These data reveal a delayed and prolonged  
121 local inflammatory response to tendon overuse characterized by an overwhelming predominance of pro-  
122 inflammatory eicosanoids and a relative lack of specialized pro-resolving lipid mediators.

#### 124 **Key words:**

125 Tendon, Lipid mediator, Eicosanoid, Inflammation, Resolution, Mass spectrometry

#### 127 **Introduction:**

128 Tendons are dense bands of connective tissue responsible for transfer of force from skeletal muscle to  
129 bone (1). Like skeletal muscle, tendons can undergo compensatory hypertrophy in response to heightened  
130 mechanical loading (2). On the other hand, repetitive tendon overuse is a major contributor to the development  
131 of tendinopathy, a common degenerative condition characterized by chronic pain and loss of function (3). Local  
132 inflammation occurs following either acute tendon injury (4-9) or repetitive overuse (10-17), but its role in the  
133 etiology of tendinopathy has been a matter of debate (18). The term tendinitis was classically used to describe  
134 symptoms of painful non-ruptured tendons, inferring key involvement of an inflammatory component (19).  
135 However, an apparent lack of polymorphonuclear leukocytes (PMNs) within diseased tendons led to the view  
136 that tendinopathy is rather a degenerative condition of tendinosis that is devoid of inflammation (20).  
137 Nevertheless, recent studies employing modern antibody based immunohistochemical staining techniques  
138 demonstrate that leukocytes, most notably monocytes/macrophages (MΦ), are indeed often present within  
139 diseased human tendons (21), stimulating a resurgence of interest into the potential role of inflammation in  
140 tendon biology (22).

141 Lipid mediators are bioactive metabolites of dietary essential polyunsaturated fatty acids (PUFA), such  
142 as omega-6 (n-6) arachidonic acid (ARA, 20:4n-6), as well as omega-3 (n-3) eicosapentaenoic acid (EPA,  
143 20:5n-3) and docosaehaenoic acid (DHA, 22:6n-3) (23). A wide-range of lipid mediators can be endogenously  
144 produced via the cyclooxygenase (COX), lipoxygenase (LOX), and epoxygenase (CYP) pathways (24). These  
This article is protected by copyright. All rights reserved

145 eicosanoids and docosanoids act as important autocrine/paracrine signaling molecules in a range of  
146 physiological processes, most notably in mediating the inflammatory response (25). Prior studies of tendon have  
147 focused overwhelmingly on the prostaglandins, classical eicosanoid metabolites generated via the COX-1 and -  
148 2 pathways (26). Local concentrations of prostaglandin E<sub>2</sub> (PGE<sub>2</sub>) are well known to increase in rodent models  
149 of either acute tendon injury (27, 28) or heightened mechanical loading (28, 29), as well as within peritendinous  
150 tissues of exercising humans (30, 31). While both PMNs (32) and MΦ (33) are major classical cellular sources  
151 of PGE<sub>2</sub>, resident tendon fibroblasts (tenocytes) also produce and release PGE<sub>2</sub> in response to either  
152 inflammatory cytokines (34) or mechanical stimulation (35).

153 Resolution of the acute inflammatory response, characterized by cessation of PMN influx and clearance  
154 of infiltrating leukocytes from the site of inflammation, was originally thought to be a passive event (36). More  
155 recently, distinct families of specialized pro-resolving mediators (SPMs) were shown to be produced during the  
156 resolution phase (37). SPM families identified to date include the ARA-derived lipoxins (e.g. LXA<sub>4</sub>) (38), EPA-  
157 derived E-series resolvins (e.g. RvE1) (39), and DHA-derived D-series resolvins (e.g. RvD1) (40), protectins  
158 (e.g. PD1) (41), and maresins (e.g. MaR1) (42). Collectively these autocooids act as endogenous stop signals to  
159 limit further PMN influx (43), while simultaneously stimulating key MΦ functions required for timely  
160 resolution and tissue repair (44). The discovery of SPMs has inspired the development of novel therapeutic  
161 strategies to modulate inflammation by mechanisms that are distinct from classical anti-inflammatory  
162 approaches such as non-steroidal anti-inflammatory drugs (NSAIDs) (45). Administration of resolution  
163 agonists, termed immunoresolvents, can limit inflammation and expedite its resolution, while simultaneously  
164 relieving pain and stimulating tissue repair (46). Unlike NSAIDs that may interfere with musculoskeletal tissue  
165 remodeling (26), remarkably immunoresolvents were recently found to rather exert overall pro-regenerative  
166 actions following skeletal muscle injury (47-52).

167 Interest into the potential role of SPMs in tendon is emerging (53). The ARA-derived SPM lipoxin A<sub>4</sub>  
168 (LXA<sub>4</sub>) (54), and its cell surface receptor (N-formyl peptide receptor 2; ALX/FPR2) (55), were both found to  
169 be increased in inflamed equine tendons and isolated human tenocytes were recently shown to produce a range  
170 of different lipid mediators *in-vitro*, including both pro-inflammatory eicosanoids and SPMs (56). Interestingly,  
171 exogenous SPM treatment could also suppress the release of pro-inflammatory cytokines by isolated human  
172 tenocytes *in-vitro*, indicative of a potential important role of these novel bioactive lipid mediators in controlling  
173 tendon inflammation (57-59). Therefore, the goal of the present study was to assess for the first time whether  
174 changes in mechanical loading of tendon modulates these endogenous inflammation-resolving pathways *in-*  
175 *vivo*.

176

177

178 **Methods:**

179

180

181

182

183

184

185

186

*Animals:* Male Sprague-Dawley rats were obtained from Charles River Laboratories and housed under specific pathogen-free conditions with ad-libitum access to food and water. Rats were used for experiments at approximately 6-months of age. Eighteen rats were randomized into each of four experimental groups, including overloaded tendons at 3 (n=4), 7 (n=4), and 28 (n=4) days following synergist ablation surgery along with a group of ambulatory control animals (n=6). Each surgical site (hind limb) was considered to be a biological replicate and each rat donated both a left and right plantaris tendon resulting in collection and analysis of 8-12 tendon samples per experimental group. All animal experiments were approved by the University of Michigan Institutional Animal Care and Use Committee (IACUC) (PRO00006079).

187

188

189

190

191

192

193

194

195

196

197

198

199

200

201

*Plantaris Tendon Overuse:* Myotectomy induced synergist ablation was used to assess the local inflammatory response to mechanical overload of the plantaris musculotendinous unit as originally described by Goldberg et al. 1967 (60). Rats were anesthetized with 2% isoflurane and preemptive analgesia provided by subcutaneous injection of buprenorphine (0.03 mg/kg) and carprofen (5 mg/kg). The skin overlying the posterior hind-limb was shaved and scrubbed with chlorhexidine and ethyl alcohol. A midline incision was made through the overlying skin and paratenon to visualize the gastrocnemius/soleus (Achilles) tendon. A full thickness tenectomy was performed to surgically remove the entire Achilles tendon mid-substance, while leaving the plantaris tendon intact. The paratenon was loosely re-approximated and the incision was closed using 4-0 Vicryl sutures. The procedure was then repeated on the contralateral limb to induce bilateral mechanical overload of both the left and right plantaris tendons. Rats were returned to their cage to recover and monitored until ambulatory with free access to food and water. Postoperative analgesia was provided via an additional single subcutaneous injection of buprenorphine (0.03 mg/kg) at 12 h post-surgery. Animals were then closely monitored daily for any signs of pain or distress for 7 days. All animals recovered well from the surgical procedure and thus no additional analgesics were administered. Age matched male rats served as non-surgical ambulatory control animals for collection and analysis of habitually loaded plantaris tendons.

202

203

204

205

206

*Tissue Collection:* Animals were euthanized via induction of bilateral pneumothorax while under deep isoflurane anesthesia. The plantaris musculotendinous unit was carefully dissected and a sample of the tendon mid-substance isolated by severing its distal insertion at the calcaneus and at its proximal border near the myotendinous junction. The isolated plantaris tendon samples were blotted dry, weighed, and then cut transversely with a scalpel blade into three separate pieces. The mid-portion of the plantaris tendon, allocated to

This article is protected by copyright. All rights reserved

immunohistochemical analysis, was oriented longitudinally on a plastic support, covered with a thin layer of optimal cutting temperature (OCT) compound, and rapidly frozen in isopentane cooled on liquid nitrogen. The remaining proximal and distal portions of the plantaris tendon, allocated to real-time quantitative reverse transcription PCR (RT-qPCR) and liquid chromatography-tandem mass spectrometry (LC-MS/MS) analysis respectively, were weighed and then snap frozen in liquid nitrogen. Samples were stored at -80°C until further analysis. Samples from the midbelly region of the plantaris muscles from these same rats were also collected for analysis and their complete mediator lipidomic profile as determined by LC-MS/MS and associated intramuscular expression of inflammation-related genes and immunohistochemical analysis of inflammatory cell infiltrates is reported in full separately (48).

***Immunohistological Analysis of Tendon Inflammation:*** A subset of n=7, n=7, n=5, and n=7 for ambulatory control, day 3, day 7, and day 28 post-synergist ablation plantaris tendons were analyzed for inflammatory cell infiltration by immunofluorescence. Tissue cross-sections (10 µm) were cut at -20°C from the mid-portion of OCT embedded plantaris tendons in a cryostat (CryoStar NX50, Thermo Fisher Scientific). Sections were adhered to SuperFrost Plus slides, air dried at room temperature, and fixed in ice-cold acetone at -20°C for 10 min. Following air drying to evaporate residual acetone the fixed slides were blocked for 1 h at room temperature in 10% normal goat serum (Invitrogen, Thermo Fisher Scientific, 10000C) in phosphate buffered saline (PBS) prior to overnight incubation at 4°C with blocking buffer containing primary antibodies raised against rat granulocytes (PMNs) (HIS48, Abcam, Ab33760, 1:20), rat CD68 (ED1, Abcam, ab31630, 1:50), and rat CD163 (ED2, Santa Cruz, sc-33560, 1:50), to simultaneously detect myeloid cell populations including PMNs, M1-like MΦ, and M2-like MΦ respectively. The following day, slides were washed in PBS and then incubated for 1 h at room temperature with secondary antibodies including Goat Anti-Mouse IgG1 Alexa Fluor 488 conjugate (Invitrogen, Thermo Fisher Scientific, A21121, 1:500 in PBS), Goat Anti-Mouse IgM Alexa Fluor 555 conjugate (Invitrogen, Thermo Fisher Scientific, A21426, 1:500 in PBS), and Goat Anti-Rabbit IgG (H+L) Alexa Fluor 647 conjugate (Invitrogen, Thermo Fisher Scientific, A21245, 1:500 in PBS). Wheat germ agglutinin (WGA) CF405S conjugate (Biotium, 29027, 100 µg/mL in PBS) was also included in the secondary antibody incubation in order to label and visualize the extracellular matrix. Following further washing in PBS, slides were mounted using Fluorescence Mounting Medium (Agilent Dako, S302380) and allowed to dry overnight protected from light at room temperature. Fluorescent images were captured using a Nikon A1 inverted confocal microscope. Tissue cross-sections (10 µm) of the plantaris muscle midbelly were prepared in parallel under identical conditions as a positive control as previously described (48).

***LC-MS/MS Based Metabolipidomic Profiling of Tendon:*** Plantaris tendon samples were mechanically homogenized in 1 mL of phosphate buffered saline (PBS) using a bead mill. The tissue homogenates were

This article is protected by copyright. All rights reserved



centrifuged at  $3000 \times g$  for 5 min and the resulting supernatant collected. Supernatants (0.85 ml) were spiked with 150  $\mu$ l methanol containing 5 ng each of 15(S)-HETE-d8, 14(15)-EpETrE-d8, Resolvin D2-d5, Leukotriene B4-d4, and Prostaglandin E1-d4 as internal standards for recovery and quantitation and mixed thoroughly. The samples were then extracted for PUFA metabolites using C18 solid phase extraction columns as previously described (48, 49, 61, 62). Briefly, the internal standard spiked samples were applied to conditioned C18 cartridges, washed with 15% methanol in water followed by hexane and then dried under vacuum. The cartridges were eluted with 2 x 0.5 ml methanol with 0.1% formic acid and then the eluate was dried under a gentle stream of nitrogen. The residue was re-dissolved in 50  $\mu$ l methanol-25 mM aqueous ammonium acetate (1:1) and subjected to LC-MS analysis. High Performance Liquid Chromatography (HPLC) was performed on a Prominence XR system (Shimadzu) using Luna C18 (3  $\mu$ m, 2.1  $\times$  150 mm) column as previously described (63, 64). The HPLC eluate was directly introduced to electrospray ionization source of a QTRAP 5500 mass analyzer (ABSCIEX) in the negative ion mode and monitored by a Multiple Reaction Monitoring (MRM) method to detect unique molecular ion – daughter ion combinations for each of the lipid mediators using a scheduled MRM around the expected retention time for each compound. Spectra of each peak detected in the scheduled MRM were recorded using Enhanced Product Ion scan to confirm the structural identity. The data were collected using Analyst 1.7 software and the MRM transition chromatograms were quantitated by MultiQuant software (both from ABSCIEX). The internal standard signals in each chromatogram were used for normalization, recovery, as well as relative quantitation of each analyte.

LC-MS/MS data was analyzed using MetaboAnalyst 4.0 (65). Analytes with >50% missing values were removed from the data set and remaining missing values were replaced with half of the minimum positive value in the original data set. Heat maps were generated in MetaboAnalyst 4.0 using the Pearson distance measure and the Ward clustering algorithm following auto scaling of features without data transformation. Volcano and principle component analysis (PCA) plots were generated using R software following  $\text{Log}_2$  data transformation using the EnhancedVolcano and FactoMineR/factoextra packages respectively

**RNA Extraction and RT-qPCR:** Tendon samples were homogenized for 45 seconds at 4 m/s in 600  $\mu$ L TRIzol reagent using a Fisherbrand™ Bead Mill 4 Homogenizer (Thermo Fisher Scientific, 15-340-164) with reinforced 2 mL screw cap tubes (Thermo Fisher Scientific, 15-340-162) and 2.4 mm metal beads (4 beads/tube) (Thermo Fisher Scientific, 15-340-158). RNA was isolated by Phenol/Chloroform extraction and RNA yield determined using a NanoDrop Spectrophotometer (Nanodrop 2000c, Thermo Fisher Scientific). Genomic DNA was removed by incubation with DNase I (Ambion, Thermo Fisher Scientific, AM2222) followed by its heat inactivation. Total RNA (250 ng) was then reverse transcribed to cDNA using SuperScript™ VILO™ Master Mix (Invitrogen, 11-755-050). RT-qPCR performed on a CFX96 Real-Time

271 PCR Detection System (Bio-Rad, 1855195) in duplicate 20  $\mu$ L reactions of iTaq™ Universal SYBR® Green  
272 Supermix (Bio-Rad, 1725124) with 1  $\mu$ M forward and reverse primers (Table 1). Relative mRNA expression  
273 was determined using the  $2^{-\Delta\Delta CT}$  method with *B2m* serving as an endogenous control.

274 **Statistics:** Data is presented as the mean  $\pm$  SEM with raw data from each individual tendon sample  
275 shown. Statistical analysis was performed in GraphPad Prism 7. Two-tailed paired t-tests were used to compare  
276 muscle and tendon samples obtained from the same rats. Between group differences were tested by two-tailed  
277 unpaired t-tests (2 groups) or by a one-way analysis of variance (ANOVA) followed by pair-wise Holm-Sidak  
278 post-hoc tests ( $\geq 3$  groups). For time-course experiments, multiple comparison testing was made compared to a  
279 single control group of tendons obtained from ambulatory control rats that did not undergo surgery.  $p \leq 0.05$  was  
280 used to determine statistical significance.

281  
282  
283  
284  
285  
286  
287  
288  
289  
290  
291  
292  
293  
294  
295  
296 **Results:**

## 297 Lipid Mediator Profile of Tendon

298 We initially examined the basal lipid mediator profile of tendon via LC-MS/MS based targeted  
 299 metabolipidomics. A total of sixty-four individual lipid mediator species were reliably detected (signal to noise  
 300 ratio >3 and peak quality >0.2 in at least 50% of samples) in plantaris tendon homogenates from ambulatory  
 301 control rats (Figure 1A). These included many bioactive metabolites of n-6 ARA derived via the COX-1 and 2  
 302 pathways [prostaglandins (PG), e.g. PGD<sub>2</sub>, PGE<sub>2</sub>, PGF<sub>2α</sub>, PGI<sub>2</sub> [measured as its inactive non-enzymatic  
 303 hydrolysis product 6-keto-PGF<sub>1α</sub> (6kPGF<sub>1α</sub>)] and thromboxanes (TX) [e.g. TXA<sub>2</sub> (measured as its inactive non-  
 304 enzymatic hydrolysis product TXB<sub>2</sub>) and the related thromboxane synthase metabolite 12-hydroxy-  
 305 heptadecatrienoic acid (12-HHTrE)] (Figure 1A, Supplemental Table 1A). Monohydroxylated ARA metabolites  
 306 of the three major mammalian lipoxygenase enzymes (5-, 12, and 15-LOX) were also detected including 5-, 12-  
 307 , 15-hydroxy-eicosatetraenoic acids (HETEs)] (Figure 1A, Supplemental Table 1B). Finally, many ARA  
 308 metabolites of the epoxygenase (CYP) pathway were present in tendon including 5(6)-, 11(12)-, 14(15)-epoxy-  
 309 eicosatrienoic acid regioisomers (EpETrEs) and corresponding downstream dihydroxy-eicosatrienoic acids  
 310 (DiHETrEs) (Figure 1A, Supplemental Table 1C). In addition to these eicosanoids, several metabolites of the  
 311 parent n-6 PUFA linoleic acid (LA, 18:2n-6) were highly abundant in tendon homogenates, including those  
 312 derived via both the LOX pathway [9- and 13-hydroxy-octadecadienoic acid (HODEs) and downstream oxo-  
 313 octadecadienoic acids (OxoODEs)] and CYP pathway [9(10)- and 12(13)-epoxy-octadecenoic acids (EpOMEs)  
 314 and downstream dihydroxy-octadecenoic acids (DiHOMEs)] (Figure 1A).

315 Many n-3 PUFA metabolites were also detected in tendon, albeit generally at relatively lower  
 316 concentrations than the above n-6 PUFA products. This included the DHA-derived SPM, resolvins D1 (RvD1),  
 317 as well as 17-hydroxy-docosahexaenoic acid (17-HDoHE), the primary intermediate 15-LOX metabolite of n-3  
 318 DHA produced during the initial step of D-series resolvins biosynthesis. Other SPMs including the E-series  
 319 resolvins (e.g. RvE1), protectins (e.g. PD1), and maresins (e.g. MaR1) were generally below the limits of  
 320 detection in tendon homogenates from ambulatory rats, although the maresin pathway marker 14-hydroxy-  
 321 docosahexaenoic acid (14-HDoHE) was detected (Supplemental Table 1D). Finally, some CYP pathway  
 322 derived epoxides of n-3 PUFAs including EPA [17(18)-epoxy-eicosatetraenoic acid (EpETEs)] and DHA [7(8)-  
 323 , 10(11)-, 13(14)-, and 16(17)-epoxy-docosapentaenoic acid (EpDPEs)] were also present within tendons of  
 324 ambulatory rats. These data reveal a wide range of novel bioactive lipid mediators within healthy tendons *in-*  
 325 *vivo* for the first time.

## 326 Functionally Associated Musculoskeletal Tissues Exhibit Highly Distinct Metabolipidomic Profiles

327 The complete LC-MS/MS profile of midbelly plantaris skeletal muscle samples from these same rats has  
328 been previously published (48). Unsupervised principle component analysis (PCA) score plots revealed that the  
329 mediator lipidome of the tendon samples analyzed here was highly distinct from that of matching plantaris  
330 muscle samples from these same ambulatory control rats (Figure 1B). Corresponding loading plots displaying  
331 some representative lipid mediators from each major enzymatic biosynthetic pathway that defined the distinct  
332 lipid mediator profiles of plantaris muscle and tendon samples are shown in Figure 1C. When pooled over these  
333 major biosynthetic pathways, 72% of the overall mediator lipidome of muscle comprised CYP pathway  
334 metabolites (e.g. EpETrEs, EpETEs, and EpDPEs), with only 7%, 10%, and 3% of total metabolites derived  
335 from the COX (e.g. PGE<sub>2</sub>), 12-LOX (e.g. 12-HETE), and 15-LOX (e.g. 15-HETE) pathways respectively  
336 (Figure 1D). In contrast, the tendon mediator lipidome overwhelmingly comprised COX (42%), 12-LOX  
337 (28%), and 15-LOX (6%) pathway metabolites, with only 9% of total lipid mediators derived from the CYP  
338 pathway (Figure 1D). Despite these differences in the relative composition of mediator lipidome between  
339 tissues, total lipid mediator concentration was similar between muscle and tendon when normalized to tissue  
340 mass (~1.2 pmol/mg) (Figure 1 D-E).

341 Parametric statistical analysis revealed that of the total seventy individual lipid mediators that were  
342 reliably detected (signal to noise ratio >3 and peak quality >0.2 in at least 50% of samples) in either tendon or  
343 muscle tissue, thirty-three were significantly enriched in tendon ( $p < 0.05$  and >1.5-fold), while eighteen were  
344 significantly enriched in muscle ( $p < 0.05$  and >1.5-fold) (Figure 1F, Supplemental Table 2A). When compared  
345 to muscle, tendon contained relatively lower absolute concentrations of anti-inflammatory CYP pathway  
346 metabolites including epoxide products of ARA [5(6)-, 8(9)-, 11(12)-, and 14(15)-EpETrEs], EPA [ 17(18)-  
347 EpETE], and DHA [7(8)-, 10(11)-, 13(14)-, 16(17)-, and 19(20)-EpDPEs]. 20-HETE, a  $\omega$ -hydroxylase CYP  
348 metabolite of ARA was similarly lacking in tendon. Finally, the primary n-3 EPA product produced during  
349 biosynthesis of the E-series resolvins, 18-HEPE, which is endogenously derived via the CYP pathway (66), was  
350 also lower in tendon than muscle. On the other hand, tendon contained far higher concentrations than muscle of  
351 many COX pathway metabolites including the major ARA-derived thromboxanes (TXB<sub>2</sub> and 12-HHTrE) and  
352 prostaglandins (PGD<sub>2</sub>, PGE<sub>2</sub>, PGF<sub>2 $\alpha$</sub> , 6-keto-PGF<sub>1 $\alpha$</sub> ). Many downstream secondary and tertiary prostaglandin  
353 metabolites of the 15-hydroxy-prostaglandin dehydrogenase (15-PGDH) and 15-oxo-prostaglandin  $\Delta^{13}$ -  
354 reductase pathways including 15-keto PGE<sub>2</sub>, 15-keto PGF<sub>2 $\alpha$</sub> , 13,14-dihydro-15-keto PGE<sub>2</sub>, and 11-dihydro-2,3-  
355 dinor TXB<sub>2</sub> were also enriched in tendon, as was the cyclopentenone prostaglandin PGJ<sub>2</sub> (which is non-  
356 enzymatically derived from PGD<sub>2</sub>). Many LOX-pathway metabolites including 5-, 11-, 12-, and 15-HETEs, 12-  
357 and 15-oxoETEs, 11-, 12-, and 15-HEPEs, 9- and 13-HODEs, 9- and 13-HOTrEs, and 5S,12S-DiHETE were  
358 also relatively enriched in tendon. Consistently, the DHA-derived SPM RvD1, which is produced by the

359 sequential action of the 15- and 5-LOX pathways, was detected in tendons of ambulatory rats, but was below  
360 the limits of detection in matching rat plantaris muscle homogenates (as previously reported) (48). A complete  
361 list of detected musculotendinous lipid mediators, magnitude of difference between tendon vs. muscle samples,  
362 associated p-values, and false discovery rates is presented in Supplemental Table 2A-D.

### 363 **Local Shifts in Lipid Mediator Biosynthesis in Response to Synergist Ablation-Induced Tendon Overuse**

364 In order to examine local shifts in lipid mediator biosynthesis in response to tendon overuse, we  
365 surgically removed the gastrocnemius/soleus (Achilles) tendon to induce compensatory mechanical overload  
366 upon the synergistic plantaris musculotendinous unit. Functionally overloaded plantaris tendons were then  
367 collected for analysis by LC-MS/MS at 3-, 7-, and 28-days following synergist ablation surgery (Figure 2).

368 When compared to control plantaris tendons obtained from age- and sex-matched ambulatory rats,  
369 intratendinous concentrations of twenty individual lipid mediator species were significantly modulated at day 3  
370 of synergist ablation-induced plantaris tendon overuse (Figure 2A, Supplemental Table 3A). This included  
371 increased concentrations of the COX/thromboxane synthase products TXB<sub>2</sub> and 12-HHTrE, as well as the  
372 COX/prostaglandin E synthase product, PGE<sub>2</sub>, as well as its downstream enzymatic inactivation products 15-  
373 keto PGE<sub>2</sub> and 13,14-dihydro-15-keto PGE<sub>2</sub>. The COX/prostaglandin D synthase product PGD<sub>2</sub> was  
374 simultaneously reduced by 50%, while COX/prostaglandin F and I synthase products PGF<sub>2 $\alpha$</sub>  and PGI<sub>2</sub>  
375 (measured as 6-keto-PGF<sub>1 $\alpha$</sub> ) remained unchanged in parallel at this time-point. Primary 15-LOX metabolites of  
376 ARA (15-HETE) and EPA (15-HEPE) were additionally increased at day 3 post surgery, with a similar non-  
377 significant trend also seen for 17-HDoHE (p=0.14), the analogous 15-LOX product of n-3 DHA. In contrast,  
378 most major metabolites of the 5-LOX (e.g. 5-HETE), 12-LOX (e.g. 12-HETE), and CYP (e.g. EpETrEs)  
379 pathways remained unchanged in tendon at day 3 following synergist ablation.

380 A total of thirty-eight lipid mediators were significantly modulated following 7 days of tendon overuse  
381 (Figure 2B, Supplemental Table 3B). This included further increases in many of the same lipid mediators seen  
382 at day 3 (e.g. TXB<sub>2</sub>, PGE<sub>2</sub>, 15-HETE) as well as additional more delayed increases in PGD<sub>2</sub> and its downstream  
383 enzymatic inactivation product 13,14-dihydro-15-keto PGD<sub>2</sub>. Similarly, PGF<sub>2 $\alpha$</sub>  and its downstream enzymatic  
384 inactivation products 15-keto-PGF<sub>2 $\alpha$</sub>  and 13,14-dihydro-15-keto PGF<sub>2 $\alpha$</sub>  were increased, as was the fifth primary  
385 prostanoid PGI<sub>2</sub> (measured as 6-keto-PGF<sub>1 $\alpha$</sub> ). Finally, the Series-J cyclopentenone prostaglandins, including  
386 PGJ<sub>2</sub>,  $\Delta^{12}$ -PGJ<sub>2</sub>, (D12-PGJ<sub>2</sub>) and 15-deoxy- $\Delta^{12,14}$ -PGJ<sub>2</sub> (15d-D12,14-PGJ<sub>2</sub>), were all produced together with  
387 their precursor PGD<sub>2</sub> at day 7 following synergist ablation (Supplemental Table 3B). The DHA-derived SPMs  
388 resolvin D2 (RvD2) and protectin D1 (PD1) additionally became detectable in tendon at day 7 of tendon  
389 overuse.

By 28-days of tendon overuse, a total of forty-nine individual lipid mediators differed significantly from ambulatory control tendons (Figure 2C, Supplemental Table 3C). This included persistent elevation of all major COX-metabolites (TXB<sub>2</sub>, PGE<sub>2</sub>, PGD<sub>2</sub>, PGF<sub>2α</sub>, and 6-keto-PGF<sub>1α</sub>) and their respective downstream metabolic inactivation products of the 15-PGDH pathway (e.g. 15-keto and 13,14-dihydro-15-keto PGs). The primary 5-LOX metabolite of n-6 ARA, 5-HETE, and its metabolite 5-oxoETE, also exhibited a delayed increase at this time-point, although related 5-LOX metabolites derived from the downstream leukotriene A<sub>4</sub> (LTA<sub>4</sub>) hydrolysis pathway, including leukotriene B<sub>4</sub> (LTB<sub>4</sub>) and 12-oxoLTB<sub>4</sub>, remained below the limits of detection. The lipoxin pathway marker 15-HETE remained increased together with an additional delayed increase in the E-series resolvin pathway marker 18-HEPE. Intratendinous RvD2 and PD1 remained increased in concentration while one additional SPM, resolvin D6 (RvD6), was also detected at the time-point. Finally, CYP pathway derived epoxides of n-6 ARA including 5(6)-, 11(12)-, and 14(15)-EpETrE were increased at day 28 of tendon overuse, as were some analogous CYP metabolites of EPA [14(15)- and 17(18)-EpETEs].

Average temporal shifts in absolute tendon lipid mediator concentrations when pooled over major enzymatic biosynthetic pathways are summarized in Figure 2D and the time-course kinetics of a selection of major representative individual lipid mediator species from each biosynthetic pathway in response to tendon overuse are shown in Figure 2E. The entire quantitative tendon LC-MS/MS data set for each individual lipid mediator profiled is shown in Supplemental Table 1. Significant increases over time were found for pooled metabolites of the COX, 5-LOX, 8-LOX, 15-LOX, and CYP pathway, as well as for pooled concentrations of detected bioactive SPMs (Figure 2D). Despite a more delayed increase in local concentrations of lipid mediators with anti-inflammatory and pro-resolving actions following synergist ablation, the overwhelming predominance of biosynthesis of classical pro-inflammatory COX pathway metabolites in mechanically overloaded plantaris tendon resulted in a progressive reduction in the percentage of the overall mediator lipidome that was derived from the LOX, CYP and SPM pathways over time (Figure 2F). Because of this, the proportion of the overall mediator lipidome consisting of classical pro-inflammatory eicosanoids derived from the COX pathway increased from 42% in control plantaris tendons from ambulatory rats (Figure 1E) to encompass 54%, 74% and 60% of the mediator lipidome at day 3, 7 and 28 of tendon overuse respectively (Figure 2F).

### Local Leukocyte Responses to Tendon Overuse

To investigate the relationship between shifts in intratendinous lipid mediator concentrations as determined by LC-MS/MS based profiling and cellular inflammatory infiltrates of tendon, we performed

This article is protected by copyright. All rights reserved

immunohistochemical staining of cross-sections of ambulatory control and mechanically overloaded plantaris tendons with antibodies to detect infiltrating myeloid cell populations including PMNs (HIS48<sup>+</sup> cells), inflammatory ED1 monocytes/MΦ (CD68<sup>+</sup> cells), and resident/M2-like ED2 MΦ (CD163<sup>+</sup> cells). We first validated these antibodies on tissue cross-sections obtained from the plantaris muscle midbelly of these same rats (Figure 3). As expected (67), rat skeletal muscle contained many resident ED2 MΦ (CD68<sup>-</sup>CD163<sup>+</sup>) cells scattered throughout internal intramuscular connective tissues (e.g. perimysium and endomysium), few rare ED1 MΦ (CD68<sup>+</sup>CD163<sup>-</sup> cells), and very few if any PMNs (HIS48<sup>+</sup> cells) (Figure 3) (48). By day 3 following synergist ablation surgery, many PMNs (HIS48<sup>+</sup> cells) and ED1 MΦ (CD68<sup>+</sup>CD163<sup>-</sup>) cells had infiltrated within the overloaded plantaris muscle, followed by progressive PMN clearance and a transition to a predominance of MΦ which co-expressed both CD68 and CD163 antigens by day 28 of recovery (Figure 3) (48). Additional representative image examples and quantitative analysis of these intramuscular myeloid cell populations in ambulatory and mechanically overloaded plantaris muscles of these same rats is published separately (48).

Unlike skeletal muscle, plantaris tendon cross-sections from ambulatory rats were apparently devoid of any resident leukocytes based on cellular protein expression of these markers both within the dense tendon core and throughout its periphery (e.g. the epitenon) under identical conditions when stained in parallel (Figure 4). At day 3 of tendon overuse there was an accumulation of many PMNs (HIS48<sup>+</sup> cells) (Figure 4A and 4B) and ED1 MΦ (CD68<sup>+</sup>CD163<sup>-</sup> cells) (Figure 4A and 4C) throughout the expanded tissue space at the plantaris tendon periphery. ED1 MΦ were also be seen within the peripheral edges of the dense tendon core at this time-point, appearing to originate from within the epitenon (Figure 5A). At this time-point, a more modest increase in the histological presence of ED2 MΦ (CD68<sup>-</sup>CD163<sup>+</sup> cells) was also seen throughout the tendon periphery (Figure 4A and 4D), but not the tendon core (Figure 5A). By day 7 of tendon overuse, there was a robust histological presence of large numbers of ED1 MΦ (CD68<sup>+</sup>CD163<sup>-</sup> cells) throughout the newly forming connective tissue layer that surrounded the original tendon (e.g. the neotendon matrix), although ED2 MΦ were no longer significantly increased (Figure 4A). Many ED1 MΦ (but not ED2 MΦ) were also seen scattered throughout the dense original tendon core at day 7 following synergist ablation (Figure 5A). By day 28 of tendon overuse, few infiltrating myeloid cells remained, in particular within the tendon core (Figure 5A). Nevertheless, some CD68<sup>+</sup>CD163<sup>-</sup> cells could still be seen scattered throughout the peripheral neotendon matrix in the majority of samples analyzed (Figure 4A and 4C). Unlike in the overloaded plantaris muscle in which there was an obvious increase in the number of MΦ co-expressing both CD68 and CD163 antigens over time (Figure 3) (48), few if any of the CD68<sup>+</sup> cells within mechanically overloaded tendons co-expressed the CD163 antigen at all time-points between day 3 and 28 of tendon overuse (Figure 4A and 5A).

### Expression of Inflammation-Related Genes in Tendon Following Synergist Ablation

453 Despite the apparent lack of histological presence of resident myeloid cells in tendon, mRNA encoding  
454 the general myeloid cell marker CD11b (*Itgam*), inflammatory monocyte/MΦ markers CD68 (*Cd68*) and EMR1  
455 (the rat analog of F4/80, *Adgre1*), as well as the resident/M2-like MΦ markers CD163 (*Cd163*) and CD206  
456 (*Mrc1*) were expressed at low but detectable levels in plantaris tendons from ambulatory rats (Figure 6).  
457 Following synergist ablation surgery, tendon mRNA expression of CD11b was increased 10-fold above  
458 ambulatory control tendons at day 3, remained elevated by 3.5 fold at day 7, but no longer differed from control  
459 levels by day 28 (Figure 6A). Similarly, expression of the MΦ markers CD68 (Figure 6B) and F4/80 (Figure  
460 6C) both increased 15-fold and 10-fold respectively at day 3, remained increased by 3.5-fold at day 7, but had  
461 returned to basal levels by day 28 of recovery. CD163 mRNA did not differ significantly from control tendons  
462 at any time-point, but was 3.5 fold higher at day 3 of tendon overuse when compared to day 28 of recovery  
463 ( $p=0.023$ ) (Figure 6D). The alternate M2-like MΦ marker CD206 (*Mrc1*) was also increased 5-fold at day 3  
464 following synergist ablation, but no longer differed from control tendons at either day 7 or 28 (Figure 6E).  
465 Expression of both the constitutive COX-1 (*Ptgs1*) and inducible COX-2 (*Ptgs2*) isoform mRNA was detectable  
466 in ambulatory control plantaris tendons. At day 3 of tendon overuse, COX-2 mRNA expression was increased  
467 by 4-fold (Figure 6G), but COX-1 mRNA remained unchanged (Figure 6F). Neither COX-1 nor COX-2 mRNA  
468 expression differed significantly from control tendons by day 7 or 28 of continued tendon overuse.

### 469 **Changes in Tendon Mass and Total RNA Content in Response to Mechanical Overuse**

470 Total RNA concentration (ng/mg of tissue) of the plantaris tendon was increased by 3.5 fold at 3 days of  
471 overuse, while tendon mass remained unchanged (Table 2). This resulted in a 3-fold increase in the total RNA  
472 content of the overloaded plantaris tendon ( $\mu\text{g RNA/tendon}$ ). Both intratendinous RNA concentration and total  
473 tendon RNA content remained increased at seven days of overuse, while tendon mass was still not yet  
474 significantly altered (1.7-fold,  $p=0.17$ ). By 28 days following synergist ablation a significant increase in the  
475 mass of the overloaded plantaris tendon was observed (2.2-fold). At this time-point, intratendinous RNA  
476 concentration no longer differed from that of ambulatory control tendons, but the total RNA content of the  
477 overloaded plantaris tendon remained increased by approximately 3-fold.



## Discussion

Here we profiled local changes in lipid mediator biosynthesis following synergist ablation-induced plantaris tendon overuse. A wide range of bioactive metabolites of the COX, LOX, and CYP pathways were detected in tendon for the first time. When compared to skeletal muscle, tendons were enriched in classical pro-inflammatory eicosanoid metabolites of the COX and 12-LOX pathways, but relatively lacking in CYP-pathway derived anti-inflammatory lipid epoxides. Three days of tendon overuse induced a robust local inflammatory response characterized by heightened biosynthesis of PGE<sub>2</sub> and TXB<sub>2</sub>, increased expression of inflammation-related genes, and peritendinous infiltration of both PMNs and MΦ. There was more delayed production of PGD<sub>2</sub>, PGF<sub>2α</sub>, 6-keto-PGF<sub>1α</sub> at day 7 at which time MΦ became the predominant myeloid cell type within tendon. Biosynthesis of some specialized pro-resolving mediators including RvD2, RvD6, and PD1 was also increased following tendon overuse, as were pathway markers of the lipoxins (15-HETE), E-resolvins (18-HEPE), and D-resolvins/protectins (17-HDoHE); however, there was a persistent reduction in the ratio of pooled SPMs and their related LOX- and CYP-derived pathway markers relative to the COX-derived prostaglandins over time. This overwhelming predominance of pro-inflammatory eicosanoids in tendon was associated with incomplete resolution of inflammation even at 28 days following synergist ablation.

The marked increase in PGE<sub>2</sub> in response to plantaris tendon overuse observed in the current study supports prior studies showing that local PGE<sub>2</sub> concentrations increase in response to an acute bout of exercise in both mice (28, 29) and humans (30, 31). While most prior studies in tendon have focused exclusively on PGE<sub>2</sub>, we show for the first time that overloaded tendons also produce substantial amounts of the other three major prostaglandins, PGD<sub>2</sub>, PGF<sub>2α</sub>, and PGI<sub>2</sub> (measured as 6-keto-PGF<sub>1α</sub>). Biosynthesis of TXA<sub>2</sub>, the fifth major primary bioactive metabolite of the COX pathway, was also increased in response to synergist ablation (based on measurement of TXB<sub>2</sub>), which is consistent with an earlier human study in which peritendinous TXB<sub>2</sub> increased following a single bout of exercise (68). Major cellular sources of specific prostanoids include blood platelets (TXA<sub>2</sub>) (69), PMNs (TXA<sub>2</sub> and PGE<sub>2</sub>) (70), mast cells (PGD<sub>2</sub>) (71) monocytes/MΦ (PGE<sub>2</sub>) (72), and vascular endothelial cells (PGI<sub>2</sub>) (73). Thus, it is likely that the PMNs and/or MΦ that accumulated in tendon in

513 the current study contributed substantially to the intratendinous prostaglandin response to mechanical overload.  
514 Although not assayed here, mast cells have also been found to appear locally in response to tendon overuse in  
515 prior studies and may thus contribute substantially to the PGD<sub>2</sub> response (11, 16). In addition to leukocytes,  
516 fibroblasts themselves can also produce prostaglandins, most notably PGE<sub>2</sub> (74), but also PGI<sub>2</sub> (75) and TXA<sub>2</sub>  
517 (76). Indeed, resident tendon fibroblasts (tenocytes) express both COX-1 and 2 (77), enabling them to locally  
518 produce and release PGE<sub>2</sub> in response to mechanical stimulation *in-vitro* (78). Consistent with our data, recent  
519 studies employing LC-MS/MS based lipid mediator profiling show that human tenocytes cultured *in-vitro* also  
520 produce substantial amounts of the other major prostanoids (PGE<sub>2</sub> > PGD<sub>2</sub> > PGF<sub>2α</sub> > TXB<sub>2</sub>) (56-59). Although  
521 PGI<sub>2</sub> does not appear to be a major product of isolated healthy tenocytes cultured *in-vitro*, stromal cells isolated  
522 from diseased human tendons do produce large amounts of PGI<sub>2</sub> (79). While tendon cells can themselves  
523 synthesize prostaglandins, even in the absence of inflammation, mechanically stimulated tenocytes release far  
524 greater amounts of PGE<sub>2</sub> when allowed to interact with MΦ than when cultured in isolation (35). Therefore,  
525 cross-talk between infiltrating myeloid cell populations such as PMNs and MΦ with resident tendon cells likely  
526 drives the robust prostaglandin response to tendon overuse.

527 While all major prostanoids were responsive to tendon overuse in the current study, notably they  
528 exhibited distinct class-specific temporal responses. Peak PMN infiltration at day 3 of tendon overuse was  
529 accompanied by a rapid initial increase in production of PGE<sub>2</sub> and TXB<sub>2</sub>, while PGD<sub>2</sub> was simultaneously  
530 reduced. Subsequently, PGD<sub>2</sub> exhibited a more delayed increase from this initial decline to reach concentrations  
531 4-fold above ambulatory controls by day 7 of tendon overuse, at which time the series-J cyclopentenone  
532 prostaglandins including PGJ<sub>2</sub>, Δ<sup>12</sup>-PGJ<sub>2</sub>, 15d-PGJ<sub>2</sub> [which are non-enzymatically derived from PGD<sub>2</sub> (80)]  
533 were also increased. In contrast to PGE<sub>2</sub>, which primarily stimulates inflammation (81), PGD<sub>2</sub> rather exerts anti-  
534 inflammatory actions directly via the DP1 prostanoid receptor, as well as secondary to the formation of  
535 downstream cyclopentenone prostaglandins such as 15d-PGJ<sub>2</sub> which are purported endogenous peroxisome  
536 proliferator-activated receptor (PPAR) ligands (82). Thus, overall our data are consistent with prior studies  
537 demonstrating a transition from a pro-inflammatory, PGE<sub>2</sub>-dominated eicosanoid profile during the  
538 development of inflammation to a more anti-inflammatory, PGD<sub>2</sub>/cyclopentenone-dominated eicosanoid profile  
539 during the resolution phase (83).

540 Earlier studies suggested that in addition to prostaglandins, tenocytes may also release the pro-  
541 inflammatory 5-LOX pathway product LTB<sub>4</sub> (78, 84). LTB<sub>4</sub> biosynthesis involves the initial formation of 5-  
542 hydroperoxy-eicosatetraenoic acid (5-HpETE) via the 5-LOX pathway, which is then converted to leukotriene  
543 A<sub>4</sub> (LTA<sub>4</sub>) by the further action of 5-LOX. In cells that express LTA<sub>4</sub> hydrolase, LTA<sub>4</sub> undergoes subsequent  
544 conversion to LTB<sub>4</sub>. Alternatively, 5-HpETE can undergo further metabolism via reduction or dehydration to 5-

545 HETE and 5-oxoETE, respectively. Both 5-HETE and 5-oxoETE were markedly increased in tendon in  
546 response to synergist ablation in the current study, but LTB<sub>4</sub> and its downstream inactivation product 12-oxo  
547 LTB<sub>4</sub> were both below the limits of detection. These data show that heightened mechanical loading of tendon *in-*  
548 *vivo* clearly does increase local biosynthesis of 5-LOX metabolites but question whether LTB<sub>4</sub> is a major  
549 metabolite produced in tendon. Consistently, recent studies by others utilizing LC-MS/MS also failed to detect  
550 LTB<sub>4</sub> in isolated human tenocytes *in-vitro* (56-58).

551 In addition to producing pro-inflammatory leukotrienes, the LOX pathways play important roles in the  
552 formation of recently identified SPM families of lipid mediators with pro-resolving actions (85). For example,  
553 lipoxin biosynthesis involves the initial production of 15-HETE, a 15-LOX metabolite of n-6 ARA, which is  
554 then released and taken up by 5-LOX expressing cells (e.g. PMNs) to be converted to LXA<sub>4</sub> and LXB<sub>4</sub> (86, 87).  
555 In analogous n-3 PUFA generated pathways, 17-HDoHE (a 15-LOX metabolite of n-3 DHA) and 18-HEPE (a  
556 CYP metabolite of n-3 EPA) are converted to the D-series resolvins (88) and E-resolvins (66) respectively via  
557 the sequential action of 5-LOX. Finally, 14-HDoHE (a 12-LOX metabolite of DHA) serves as the primary  
558 intermediate produced during biosynthesis of the most recently identified maresin family of SPMs (42). We  
559 show here that tendon contains detectable levels of all four of these major monohydroxylated SPM pathway  
560 markers. Tendon overuse markedly increased local concentrations of 15-HETE, 18-HEPE, and 17-HDoHE. On  
561 the other hand, 14-HDoHE was unchanged in response to tendon overuse, as were the related 12-LOX  
562 metabolites of ARA (12-HETE) and EPA (12-HEPE). Overall these data show that, CYP and 15-LOX derived  
563 SPM biosynthetic pathways are induced in the mechanically overloaded plantaris tendon, like they are in  
564 functionally associated muscle (48). In contrast, metabolites of the 12-LOX pathway which are major  
565 metabolites produced within functionally overloaded skeletal muscle (48, 49), do not appear to be responsive to  
566 heightened mechanical loading of tendon.

567 We also detected RvD1 in tendon, but its concentration was apparently not influenced by tendon  
568 overuse. In contrast, RvD2, PD1, and RvD6 were below the limits of detection in tendons from ambulatory rats,  
569 but did increase in concentration to become detectable following synergist ablation. Other mature SPMs  
570 including the lipoxins (LXA<sub>4</sub> and LXB<sub>4</sub>), E-series resolvins (RvE1 and RvE3), and maresins (MaR1) were  
571 generally below the limits of detection of our LC-MS/MS assay in tendon irrespective of time-point. Overall  
572 our data are consistent with recent work showing that isolated human tendon stromal cells cultured *in-vitro* may  
573 produce LOX-derived SPMs, in addition to classical pro-inflammatory eicosanoids (56-58). However, similar to  
574 the case with skeletal muscle tissue (48, 49), tendon homogenates *in-vivo* clearly contain far greater  
575 concentrations of primary LOX and CYP derived monohydroxylated intermediates in SPM pathways than the  
576 bioactive SPMs themselves. This may be attributable to the highly transient nature of mature SPMs, their

relative enrichment in the extracellular vs intracellular environment, and/or their naturally low concentrations relative to the limits of detection of the LC-MS/MS assay used here.

We found that plantaris tendons from ambulatory control rats were apparently devoid of resident myeloid cells. This finding is consistent with many prior studies that have reported that healthy tendons do not appear to contain a resident M $\Phi$  population (9, 10, 14-17, 55, 89). In contrast, a recent study described the presence of a novel population of ‘tenophages’ residing within the dense core of Achilles tendons of healthy ambulatory mice that expressed M $\Phi$  lineage markers (e.g. CD68) together with the tenocyte lineage marker scleraxis (90). As a positive control (67), we could easily observe many resident ED2 M $\Phi$  (CD68<sup>-</sup>CD163<sup>+</sup> cells) scattered throughout the perimysium and endomysium of plantaris muscles from these same rats (48). Plantaris tendons did clearly contain resident cells that expressed detectable amounts of mRNA encoding these and other immune cell markers as determined by RT-qPCR. Interpretation of this finding is complicated, however, by prior studies showing that various non-myeloid cell types, including fibroblasts, may also express low levels of common myeloid lineage markers such as CD68 (91). Thus, it currently remains unclear whether a bonafide resident M $\Phi$  population exists within the dense core of the tendon proper or rather whether populations of resident tenocytes also express relatively lower amounts of markers commonly used to identify myeloid cells. If such cells do reside in the healthy tendon our data show that either the proteins are not synthesized or are very rapidly degraded resulting in expression levels of these markers far lower than those M $\Phi$  that are well-established to reside within the extracellular matrix of skeletal muscle (48, 67).

Unlike in tendons from ambulatory rats, we observed a robust peritendinous infiltration of both PMNs and M $\Phi$  following synergist ablation surgery. These data are consistent with early studies in which repetitive kicking exercise in rabbits was shown to result in Achilles paratendinitis (13, 92). In a series of later studies inflammatory ED1 monocytes/M $\Phi$  (CD68<sup>+</sup> cells) were also shown to infiltrate peritendinous tissues of the upper limb in response to repetitive reaching/grasping activity in rats (14-17). While PMNs were specifically localized to the tendon periphery, interestingly we did observe a more delayed increase in M $\Phi$  within the dense tendon core in the current study. This finding is consistent with a recent report in which CD68<sup>+</sup> cells were shown to infiltrate within the core of the Achilles tendon proper following 3-weeks of daily intensive treadmill running in mice (10). To our knowledge, only a single prior study has quantified intratendinous ED2 M $\Phi$  (CD163<sup>+</sup> cells) in response to tendon overuse (14). In this study, repetitive upper extremity reaching and grasping in rats resulted in robust infiltration of palmar and forearm tendons by ED1 M $\Phi$  (CD68<sup>+</sup> cells) between 3-6 weeks of overuse, with no change in ED2 M $\Phi$  (CD163<sup>+</sup> cell) number at this time-point (14). Nevertheless, there was a more modest increase in ED2 M $\Phi$  (CD163<sup>+</sup> cells) in the forelimb tendons by weeks 6-8 of continued overuse (14). Overall, our results following synergist ablation appear most similar to prior studies of

intratendinous injection of collagenase, in which only a modest and transient increase in tendon CD163<sup>+</sup> cells occurred at day 3 post-injury (7, 93). However, we cannot discount the possibility that our latest time-point of 28 days post-surgery may have been too early to observe an intratendinous CD163<sup>+</sup> cell response (14).

Healthy tendon is a poorly vascularized tissue with blood supply mainly derived from anatomically associated intrinsic sites of the musculotendinous and osteotendinous junctions, as well extrinsic sites of the synovial sheath/loose areolar connective tissue (paratenon) which surrounds non-synovial tendons (94). The exclusive presence of PMNs throughout the periphery of the overloaded plantaris tendon within the epitenon/neotendon matrix suggests that these cells most likely originate via delivery from blood vessels of the paratenon. Similarly, an earlier presence of monocytes/M $\Phi$  within the epitenon/immature neotendon, followed only by their later delayed appearance in the dense tendon core, suggests that they too may have originated from within the paratenon. However, we cannot discount that the large numbers of CD68<sup>+</sup> monocytes/M $\Phi$  that rapidly invaded within the highly vascularized plantaris muscle may be an additional source of the M $\Phi$  within the tendon core, potentially via migration into tendon via the musculotendinous junction through intramuscular connective tissues (e.g. endomysium/perimysium) and/or related blood vessels (48).

A single bout of resistance exercise in humans results in a transient increase in blood serum concentrations of a large number of lipid mediators (61). Many of these same lipid mediators also transiently increase within the exercised musculature of human subjects following an acute bout of muscle damaging (eccentric) contractions, suggesting that injured muscle cells may contribute to the systemic lipid mediator response to exercise stress (62). Consistent with this hypothesis, rodent experimental models of muscle injury were recently found to markedly increase intramuscular lipid mediators (47-49). However, aerobic exercise, which is generally not thought to inflict substantial muscle damage, also results in marked increases in plasma lipid mediator concentrations (95, 96). The remarkable capacity of mechanically overloaded tendon to produce bioactive lipid mediators identified in the current study suggests that tendon may also be an important and underappreciated cellular source of systemic lipid mediator to physical exercise (97). Indeed, biopsy samples obtained from human patellar tendons were previously found to express far greater amounts of COX-1 and -2 mRNA when compared to those obtained from the quadriceps muscle (98). Earlier rodent studies also showed that tendons and associated intramuscular connective tissues expressed prostaglandin biosynthetic enzymes much more robustly than the contractile muscle cells (myofibers) that make up the bulk of muscle (99). Consistent with these prior studies, we found that the plantaris tendon homogenates analyzed here were greatly enriched in prostaglandins when compared to plantaris muscle tissue samples obtained from these same rats (48). Overall, these data suggest that muscle-associated connective tissues are likely a key cellular source of bioactive lipid mediators that may serve as autocrine/paracrine signaling molecules between tendon and/or

641 muscle fibroblasts and other functionally associated muscle and tendon cells. Similarly, muscle and/or tendon  
642 derived lipid mediators may potentially exert cross-organ endocrine actions following their systemic release  
643 from the mechanically overloaded musculotendinous unit, as has been previously demonstrated for adipose  
644 tissue derived lipid mediators (100).

645 One potential limitation of the current study is the perioperative treatment of rats with analgesics  
646 including the NSAID carprofen and the opioid buprenorphine, which was an ethical requirement to minimize  
647 post-surgical pain. NSAID treatment has been shown to block tenocyte production of PGE<sub>2</sub> *in-vitro* (35), reduce  
648 peritendinous concentrations of PGE<sub>2</sub> in human subjects (30, 101) and to limit infiltration of PMNs and ED1  
649 MΦ in injured rat tendons (102). While the potential impact of opioid treatment on tendon inflammation is less  
650 clear, some evidence exists to suggest that these drugs may also be immunosuppressive (103). Therefore, we  
651 cannot discount the possibility that the local inflammatory response to tendon overuse would have been even  
652 greater in the current study in the absence of treatment with these analgesic drugs.

653 In conclusion, we show for the first time that tendon contains a diverse array of bioactive lipid mediators  
654 derived from the COX, LOX and CYP pathways, local biosynthesis of many of which is markedly increased in  
655 response to mechanical overuse. When compared to muscle, tendons are greatly enriched in COX and LOX  
656 metabolites, but is relatively lacking in products of the CYP pathway. A rapid increase in local concentrations  
657 of TXB<sub>2</sub> and PGE<sub>2</sub> in mechanically overloaded tendons accompanies peritendinous infiltration of PMNs. The  
658 subsequent a more delayed increase in intratendinous anti-inflammatory/pro-resolving mediators is  
659 accompanied by a progressive PMN clearance and transition to a predominance of MΦ in chronically  
660 overloaded tendons. Despite this, the SPM response appears insufficient to counteract development of chronic  
661 tendon inflammation as evidenced by incomplete resolution of the inflammatory response even at 28 days of  
662 continued tendon overuse.

### 663 **Acknowledgments:**

664 This work was supported by the Glenn Foundation for Medical Research Post-Doctoral Fellowship in  
665 Aging Research (JFM), the University of Michigan Department of Orthopedic Surgery, and the National  
666 Institutes of Health (NIH) under the awards R01 (AG050676) (SVB), PO1 (AG051442) (SVB), P30  
667 (AR069620) (SVB) and S10 (RR027926) (KRM).

### 668 **Conflict of interest statement:**

669 The authors have stated explicitly that there are no conflicts of interest in connection with this article.

### 670 **Author contributions:**

This article is protected by copyright. All rights reserved

671 J.F.M conceived the study. S.V.B and K.R.M and supervised the work. J.F.M and K.B.S designed the  
672 experiments. J.F.M and D.C.S performed the experiments. J.F.M and K.R.M analyzed the data. J.F.M prepared  
673 the figures and wrote the manuscript with input from all authors.

674  
675  
676  
677  
678  
679  
680  
681  
682  
683  
684 **References:**

- 685 1. Thorpe, C. T., and Screen, H. R. (2016) Tendon Structure and Composition. *Adv Exp Med Biol* **920**, 3-  
686 10
- 687 2. Kongsgaard, M., Reitelsheder, S., Pedersen, T. G., Holm, L., Aagaard, P., Kjaer, M., and Magnusson, S.  
688 P. (2007) Region specific patellar tendon hypertrophy in humans following resistance training. *Acta*  
689 *Physiol (Oxf)* **191**, 111-121
- 690 3. Abat, F., Alfredson, H., Cucchiaroni, M., Madry, H., Marmotti, A., Mouton, C., Oliveira, J. M., Pereira,  
691 H., Peretti, G. M., Romero-Rodriguez, D., Spang, C., Stephen, J., van Bergen, C. J. A., and de Girolamo,  
692 L. (2017) Current trends in tendinopathy: consensus of the ESSKA basic science committee. Part I:  
693 biology, biomechanics, anatomy and an exercise-based approach. *J Exp Orthop* **4**, 18
- 694 4. Wojciak, B., and Crossan, J. F. (1993) The accumulation of inflammatory cells in synovial sheath and  
695 epitenon during adhesion formation in healing rat flexor tendons. *Clin Exp Immunol* **93**, 108-114
- 696 5. Kang, H. J., Park, B. M., Hahn, S. B., and Kang, E. S. (1990) An experimental study of healing of the  
697 partially severed flexor tendon in chickens. *Yonsei Med J* **31**, 264-273

- 698 6. Enwemeka, C. S. (1989) Inflammation, cellularity, and fibrillogenesis in regenerating tendon:  
699 implications for tendon rehabilitation. *Phys Ther* **69**, 816-825
- 700 7. Marsolais, D., Cote, C. H., and Frenette, J. (2001) Neutrophils and macrophages accumulate  
701 sequentially following Achilles tendon injury. *J Orthop Res* **19**, 1203-1209
- 702 8. Kawamura, S., Ying, L., Kim, H. J., Dynybil, C., and Rodeo, S. A. (2005) Macrophages accumulate in  
703 the early phase of tendon-bone healing. *J Orthop Res* **23**, 1425-1432
- 704 9. Wong, J. K., Lui, Y. H., Kapacee, Z., Kadler, K. E., Ferguson, M. W., and McGrouther, D. A. (2009)  
705 The cellular biology of flexor tendon adhesion formation: an old problem in a new paradigm. *Am J*  
706 *Pathol* **175**, 1938-1951
- 707 10. Zhao, G., Zhang, J., Nie, D., Zhou, Y., Li, F., Onishi, K., Billiar, T., and Wang, J. H. (2019) HMGB1  
708 mediates the development of tendinopathy due to mechanical overloading. *PLoS One* **14**, e0222369
- 709 11. Pingel, J., Wienecke, J., Kongsgaard, M., Behzad, H., Abraham, T., Langberg, H., and Scott, A. (2013)  
710 Increased mast cell numbers in a calcaneal tendon overuse model. *Scand J Med Sci Sports* **23**, e353-360
- 711 12. Messner, K., Wei, Y., Andersson, B., Gillquist, J., and Rasanen, T. (1999) Rat model of Achilles tendon  
712 disorder. A pilot study. *Cells Tissues Organs* **165**, 30-39
- 713 13. Backman, C., Boquist, L., Friden, J., Lorentzon, R., and Toolanen, G. (1990) Chronic achilles  
714 paratenonitis with tendinosis: an experimental model in the rabbit. *J Orthop Res* **8**, 541-547
- 715 14. Barbe, M. F., Barr, A. E., Gorzelany, I., Amin, M., Gaughan, J. P., and Safadi, F. F. (2003) Chronic  
716 repetitive reaching and grasping results in decreased motor performance and widespread tissue  
717 responses in a rat model of MSD. *J Orthop Res* **21**, 167-176
- 718 15. Kietrys, D. M., Barr-Gillespie, A. E., Amin, M., Wade, C. K., Popoff, S. N., and Barbe, M. F. (2012)  
719 Aging contributes to inflammation in upper extremity tendons and declines in forelimb agility in a rat  
720 model of upper extremity overuse. *PLoS One* **7**, e46954
- 721 16. Fedorczyk, J. M., Barr, A. E., Rani, S., Gao, H. G., Amin, M., Amin, S., Litvin, J., and Barbe, M. F.  
722 (2010) Exposure-dependent increases in IL-1beta, substance P, CTGF, and tendinosis in flexor  
723 digitorum tendons with upper extremity repetitive strain injury. *J Orthop Res* **28**, 298-307
- 724 17. Barbe, M. F., Elliott, M. B., Abdelmagid, S. M., Amin, M., Popoff, S. N., Safadi, F. F., and Barr, A. E.  
725 (2008) Serum and tissue cytokines and chemokines increase with repetitive upper extremity tasks. *J*  
726 *Orthop Res* **26**, 1320-1326
- 727 18. Abate, M., Silbernagel, K. G., Siljeholm, C., Di Iorio, A., De Amicis, D., Salini, V., Werner, S., and  
728 Paganelli, R. (2009) Pathogenesis of tendinopathies: inflammation or degeneration? *Arthritis Res Ther*  
729 **11**, 235



- 730 19. Mosca, M. J., Rashid, M. S., Snelling, S. J., Kirtley, S., Carr, A. J., and Dakin, S. G. (2018) Trends in  
731 the theory that inflammation plays a causal role in tendinopathy: a systematic review and quantitative  
732 analysis of published reviews. *BMJ Open Sport Exerc Med* **4**, e000332
- 733 20. Khan, K. M., Cook, J. L., Kannus, P., Maffulli, N., and Bonar, S. F. (2002) Time to abandon the  
734 "tendinitis" myth. *BMJ* **324**, 626-627
- 735 21. Jomaa, G., Kwan, C. K., Fu, S. C., Ling, S. K., Chan, K. M., Yung, P. S., and Rolf, C. (2020) A  
736 systematic review of inflammatory cells and markers in human tendinopathy. *BMC Musculoskelet*  
737 *Disord* **21**, 78
- 738 22. Rees, J. D., Stride, M., and Scott, A. (2014) Tendons--time to revisit inflammation. *Br J Sports Med* **48**,  
739 1553-1557
- 740 23. Gilroy, D. W., and Bishop-Bailey, D. (2019) Lipid mediators in immune regulation and resolution. *Br J*  
741 *Pharmacol* **176**, 1009-1023
- 742 24. Leuti, A., Fazio, D., Fava, M., Piccoli, A., Oddi, S., and Maccarrone, M. (2020) Bioactive lipids,  
743 inflammation and chronic diseases. *Adv Drug Deliv Rev*
- 744 25. Christie, W. W., and Harwood, J. L. (2020) Oxidation of polyunsaturated fatty acids to produce lipid  
745 mediators. *Essays Biochem*
- 746 26. Su, B., and O'Connor, J. P. (2013) NSAID therapy effects on healing of bone, tendon, and the enthesis. *J*  
747 *Appl Physiol (1985)* **115**, 892-899
- 748 27. Zhang, J., Middleton, K. K., Fu, F. H., Im, H. J., and Wang, J. H. (2013) HGF mediates the anti-  
749 inflammatory effects of PRP on injured tendons. *PLoS One* **8**, e67303
- 750 28. Zhang, J., Pan, T., and Wang, J. H. (2014) Cryotherapy suppresses tendon inflammation in an animal  
751 model. *J Orthop Translat* **2**, 75-81
- 752 29. Zhang, J., Pan, T., Liu, Y., and Wang, J. H. (2010) Mouse treadmill running enhances tendons by  
753 expanding the pool of tendon stem cells (TSCs) and TSC-related cellular production of collagen. *J*  
754 *Orthop Res* **28**, 1178-1183
- 755 30. Langberg, H., Boushel, R., Skovgaard, D., Risum, N., and Kjaer, M. (2003) Cyclo-oxygenase-2  
756 mediated prostaglandin release regulates blood flow in connective tissue during mechanical loading in  
757 humans. *J Physiol* **551**, 683-689
- 758 31. Langberg, H., Skovgaard, D., Petersen, L. J., Bulow, J., and Kjaer, M. (1999) Type I collagen synthesis  
759 and degradation in peritendinous tissue after exercise determined by microdialysis in humans. *J Physiol*  
760 **521 Pt 1**, 299-306
- 761 32. Zurier, R. B., and Sayadoff, D. M. (1975) Release of prostaglandins from human polymorphonuclear  
762 leukocytes. *Inflammation* **1**, 93-101

- 763 33. Humes, J. L., Bonney, R. J., Pelus, L., Dahlgren, M. E., Sadowski, S. J., Kuehl, F. A., Jr., and Davies, P.  
764 (1977) Macrophages synthesis and release prostaglandins in response to inflammatory stimuli. *Nature*  
765 **269**, 149-151
- 766 34. Tsuzaki, M., Guyton, G., Garrett, W., Archambault, J. M., Herzog, W., Almekinders, L., Bynum, D.,  
767 Yang, X., and Banes, A. J. (2003) IL-1 beta induces COX2, MMP-1, -3 and -13, ADAMTS-4, IL-1 beta  
768 and IL-6 in human tendon cells. *J Orthop Res* **21**, 256-264
- 769 35. Almekinders, L. C., Baynes, A. J., and Bracey, L. W. (1995) An in vitro investigation into the effects of  
770 repetitive motion and nonsteroidal antiinflammatory medication on human tendon fibroblasts. *Am J*  
771 *Sports Med* **23**, 119-123
- 772 36. Serhan, C. N. (2011) The resolution of inflammation: the devil in the flask and in the details. *FASEB J*  
773 **25**, 1441-1448
- 774 37. Serhan, C. N. (2017) Discovery of specialized pro-resolving mediators marks the dawn of resolution  
775 physiology and pharmacology. *Mol Aspects Med* **58**, 1-11
- 776 38. Serhan, C. N., Hamberg, M., and Samuelsson, B. (1984) Lipoxins: novel series of biologically active  
777 compounds formed from arachidonic acid in human leukocytes. *Proc Natl Acad Sci U S A* **81**, 5335-  
778 5339
- 779 39. Serhan, C. N., Clish, C. B., Brannon, J., Colgan, S. P., Chiang, N., and Gronert, K. (2000) Novel  
780 functional sets of lipid-derived mediators with antiinflammatory actions generated from omega-3 fatty  
781 acids via cyclooxygenase 2-nonsteroidal antiinflammatory drugs and transcellular processing. *J Exp*  
782 *Med* **192**, 1197-1204
- 783 40. Serhan, C. N., Hong, S., Gronert, K., Colgan, S. P., Devchand, P. R., Mirick, G., and Moussignac, R. L.  
784 (2002) Resolvins: a family of bioactive products of omega-3 fatty acid transformation circuits initiated  
785 by aspirin treatment that counter proinflammation signals. *J Exp Med* **196**, 1025-1037
- 786 41. Mukherjee, P. K., Marcheselli, V. L., Serhan, C. N., and Bazan, N. G. (2004) Neuroprotectin D1: a  
787 docosahexaenoic acid-derived docosatriene protects human retinal pigment epithelial cells from  
788 oxidative stress. *Proc Natl Acad Sci U S A* **101**, 8491-8496
- 789 42. Serhan, C. N., Yang, R., Martinod, K., Kasuga, K., Pillai, P. S., Porter, T. F., Oh, S. F., and Spite, M.  
790 (2009) Maresins: novel macrophage mediators with potent antiinflammatory and proresolving actions. *J*  
791 *Exp Med* **206**, 15-23
- 792 43. Chiang, N., and Serhan, C. N. (2017) Structural elucidation and physiologic functions of specialized  
793 pro-resolving mediators and their receptors. *Mol Aspects Med* **58**, 114-129
- 794 44. Dalli, J., and Serhan, C. N. (2017) Pro-Resolving Mediators in Regulating and Conferring Macrophage  
795 Function. *Front Immunol* **8**, 1400

- 796 45. Serhan, C. N. (2017) Treating inflammation and infection in the 21st century: new hints from decoding  
797 resolution mediators and mechanisms. *FASEB J* **31**, 1273-1288
- 798 46. Dalli, J., and Serhan, C. N. (2019) Identification and structure elucidation of the pro-resolving mediators  
799 provides novel leads for resolution pharmacology. *Br J Pharmacol* **176**, 1024-1037
- 800 47. Giannakis, N., Sansbury, B. E., Patsalos, A., Hays, T. T., Riley, C. O., Han, X., Spite, M., and Nagy, L.  
801 (2019) Dynamic changes to lipid mediators support transitions among macrophage subtypes during  
802 muscle regeneration. *Nat Immunol* **20**, 626-636
- 803 48. Markworth, J. F., Brown, L. A., Lim, E., Floyd, C., Larouche, J., Castor-Macias, J. A., Sugg, K. B.,  
804 Sarver, D. C., Macpherson, P. C., Davis, C., Aguilar, C. A., Maddipati, K. R., and Brooks, S. V. (2020)  
805 Resolvin D1 supports skeletal myofiber regeneration via actions on myeloid and muscle stem cells. *JCI*  
806 *Insight* **5**
- 807 49. Markworth, J. F., Brown, L. A., Lim, E., Castor-Macias, J. A., Larouche, J., Macpherson, P. C. D.,  
808 Davis, C., Aguilar, C. A., Maddipati, K. R., and Brooks, S. V. (2020) Lipidomic Profiling Reveals an  
809 Age-Related Deficiency of Skeletal Muscle Proresolving Mediators that Contributes to Maladaptive  
810 Tissue Remodeling. *bioRxiv*, 2020.2011.2005.370056
- 811 50. Sansbury, B. E., Li, X., Wong, B., Patsalos, A., Giannakis, N., Zhang, M. J., Nagy, L., and Spite, M.  
812 (2020) Myeloid ALX/FPR2 regulates vascularization following tissue injury. *Proc Natl Acad Sci U S A*  
813 **117**, 14354-14364
- 814 51. McArthur, S., Juban, G., Gobbetti, T., Desgeorges, T., Theret, M., Gondin, J., Toller-Kawahisa, J. E.,  
815 Reutelingsperger, C. P., Chazaud, B., Perretti, M., and Mounier, R. (2020) Annexin A1 drives  
816 macrophage skewing to accelerate muscle regeneration through AMPK activation. *J Clin Invest* **130**,  
817 1156-1167
- 818 52. Zhang, M. J., Sansbury, B. E., Hellmann, J., Baker, J. F., Guo, L., Parmer, C. M., Prenner, J. C.,  
819 Conklin, D. J., Bhatnagar, A., Creager, M. A., and Spite, M. (2016) Resolvin D2 Enhances Postischemic  
820 Revascularization While Resolving Inflammation. *Circulation* **134**, 666-680
- 821 53. Dakin, S. G., Dudhia, J., and Smith, R. K. (2014) Resolving an inflammatory concept: the importance of  
822 inflammation and resolution in tendinopathy. *Vet Immunol Immunopathol* **158**, 121-127
- 823 54. Dakin, S. G., Dudhia, J., Werling, N. J., Werling, D., Abayasekara, D. R., and Smith, R. K. (2012)  
824 Inflamm-aging and arachadonic acid metabolite differences with stage of tendon disease. *PLoS One* **7**,  
825 e48978
- 826 55. Dakin, S. G., Werling, D., Hibbert, A., Abayasekara, D. R., Young, N. J., Smith, R. K., and Dudhia, J.  
827 (2012) Macrophage sub-populations and the lipoxin A4 receptor implicate active inflammation during  
828 equine tendon repair. *PLoS One* **7**, e32333

- 829 56. Dakin, S. G., Ly, L., Colas, R. A., Oppermann, U., Wheway, K., Watkins, B., Dalli, J., and Carr, A. J.  
830 (2017) Increased 15-PGDH expression leads to dysregulated resolution responses in stromal cells from  
831 patients with chronic tendinopathy. *Sci Rep* **7**, 11009
- 832 57. Dakin, S. G., Colas, R. A., Newton, J., Gwilym, S., Jones, N., Reid, H. A. B., Wood, S., Appleton, L.,  
833 Wheway, K., Watkins, B., Dalli, J., and Carr, A. J. (2019) 15-Epi-LXA4 and MaR1 counter  
834 inflammation in stromal cells from patients with Achilles tendinopathy and rupture. *FASEB J* **33**, 8043-  
835 8054
- 836 58. Dakin, S. G., Colas, R. A., Wheway, K., Watkins, B., Appleton, L., Rees, J., Gwilym, S., Little, C.,  
837 Dalli, J., and Carr, A. J. (2019) Proresolving Mediators LXB4 and RvE1 Regulate Inflammation in  
838 Stromal Cells from Patients with Shoulder Tendon Tears. *Am J Pathol* **189**, 2258-2268
- 839 59. Dakin, S. G., Martinez, F. O., Yapp, C., Wells, G., Oppermann, U., Dean, B. J., Smith, R. D., Wheway,  
840 K., Watkins, B., Roche, L., and Carr, A. J. (2015) Inflammation activation and resolution in human  
841 tendon disease. *Sci Transl Med* **7**, 311ra173
- 842 60. Goldberg, A. L. (1967) Work-induced growth of skeletal muscle in normal and hypophysectomized rats.  
843 *Am J Physiol* **213**, 1193-1198
- 844 61. Markworth, J. F., Vella, L., Lingard, B. S., Tull, D. L., Rupasinghe, T. W., Sinclair, A. J., Maddipati, K.  
845 R., and Cameron-Smith, D. (2013) Human inflammatory and resolving lipid mediator responses to  
846 resistance exercise and ibuprofen treatment. *Am J Physiol Regul Integr Comp Physiol* **305**, R1281-1296
- 847 62. Vella, L., Markworth, J. F., Farnfield, M. M., Maddipati, K. R., Russell, A. P., and Cameron-Smith, D.  
848 (2019) Intramuscular inflammatory and resolving lipid profile responses to an acute bout of resistance  
849 exercise in men. *Physiol Rep* **7**, e14108
- 850 63. Maddipati, K. R., Romero, R., Chaiworapongsa, T., Zhou, S. L., Xu, Z., Tarca, A. L., Kusanovic, J. P.,  
851 Munoz, H., and Honn, K. V. (2014) Eicosanomic profiling reveals dominance of the epoxygenase  
852 pathway in human amniotic fluid at term in spontaneous labor. *FASEB J* **28**, 4835-4846
- 853 64. Norris, P. C., Skulas-Ray, A. C., Riley, I., Richter, C. K., Kris-Etherton, P. M., Jensen, G. L., Serhan, C.  
854 N., and Maddipati, K. R. (2018) Identification of specialized pro-resolving mediator clusters from  
855 healthy adults after intravenous low-dose endotoxin and omega-3 supplementation: a methodological  
856 validation. *Sci Rep* **8**, 18050
- 857 65. Chong, J., Soufan, O., Li, C., Caraus, I., Li, S., Bourque, G., Wishart, D. S., and Xia, J. (2018)  
858 MetaboAnalyst 4.0: towards more transparent and integrative metabolomics analysis. *Nucleic Acids Res*  
859 **46**, W486-W494

- 860 66. Arita, M., Clish, C. B., and Serhan, C. N. (2005) The contributions of aspirin and microbial oxygenase  
861 to the biosynthesis of anti-inflammatory resolvins: novel oxygenase products from omega-3  
862 polyunsaturated fatty acids. *Biochem Biophys Res Commun* **338**, 149-157
- 863 67. Honda, H., Kimura, H., and Rostami, A. (1990) Demonstration and phenotypic characterization of  
864 resident macrophages in rat skeletal muscle. *Immunology* **70**, 272-277
- 865 68. Langberg, H., Skovgaard, D., Karamouzis, M., Bulow, J., and Kjaer, M. (1999) Metabolism and  
866 inflammatory mediators in the peritendinous space measured by microdialysis during intermittent  
867 isometric exercise in humans. *J Physiol* **515 ( Pt 3)**, 919-927
- 868 69. Svensson, J., Hamberg, M., and Samuelsson, B. (1976) On the formation and effects of thromboxane A2  
869 in human platelets. *Acta Physiol Scand* **98**, 285-294
- 870 70. Pouliot, M., Gilbert, C., Borgeat, P., Poubelle, P. E., Bourgoin, S., Creminon, C., Maclouf, J., McColl,  
871 S. R., and Naccache, P. H. (1998) Expression and activity of prostaglandin endoperoxide synthase-2 in  
872 agonist-activated human neutrophils. *FASEB J* **12**, 1109-1123
- 873 71. Lewis, R. A., Soter, N. A., Diamond, P. T., Austen, K. F., Oates, J. A., and Roberts, L. J., 2nd. (1982)  
874 Prostaglandin D2 generation after activation of rat and human mast cells with anti-IgE. *J Immunol* **129**,  
875 1627-1631
- 876 72. Kurland, J. I., and Bockman, R. (1978) Prostaglandin E production by human blood monocytes and  
877 mouse peritoneal macrophages. *J Exp Med* **147**, 952-957
- 878 73. Weksler, B. B., Marcus, A. J., and Jaffe, E. A. (1977) Synthesis of prostaglandin I2 (prostacyclin) by  
879 cultured human and bovine endothelial cells. *Proc Natl Acad Sci U S A* **74**, 3922-3926
- 880 74. Zucali, J. R., Dinarello, C. A., Oblon, D. J., Gross, M. A., Anderson, L., and Weiner, R. S. (1986)  
881 Interleukin 1 stimulates fibroblasts to produce granulocyte-macrophage colony-stimulating activity and  
882 prostaglandin E2. *J Clin Invest* **77**, 1857-1863
- 883 75. Ali, A. E., Barrett, J. C., and Eling, T. E. (1980) Prostaglandin and thromboxane production by  
884 fibroblasts and vascular endothelial cells. *Adv Prostaglandin Thromboxane Res* **6**, 533-535
- 885 76. Bryant, R. W., Feinmark, S. J., Makheja, A. N., and Bailey, J. M. (1978) Lipid metabolism in cultured  
886 cells. Synthesis of vasoactive thromboxane A2 from [14C]arachidonic acid culture lung fibroblasts. *J*  
887 *Biol Chem* **253**, 8134-8142
- 888 77. Wang, J. H., Jia, F., Yang, G., Yang, S., Campbell, B. H., Stone, D., and Woo, S. L. (2003) Cyclic  
889 mechanical stretching of human tendon fibroblasts increases the production of prostaglandin E2 and  
890 levels of cyclooxygenase expression: a novel in vitro model study. *Connect Tissue Res* **44**, 128-133
- 891 78. Almekinders, L. C., Banes, A. J., and Ballenger, C. A. (1993) Effects of repetitive motion on human  
892 fibroblasts. *Med Sci Sports Exerc* **25**, 603-607

79. Bergqvist, F., Carr, A. J., Whewey, K., Watkins, B., Oppermann, U., Jakobsson, P. J., and Dakin, S. G. (2019) Divergent roles of prostacyclin and PGE2 in human tendinopathy. *Arthritis Res Ther* **21**, 74
80. Fitzpatrick, F. A., and Wynalda, M. A. (1983) Albumin-catalyzed metabolism of prostaglandin D2. Identification of products formed in vitro. *J Biol Chem* **258**, 11713-11718
81. Williams, T. J. (1979) Prostaglandin E2, prostaglandin I2 and the vascular changes of inflammation. *Br J Pharmacol* **65**, 517-524
82. Rajakariar, R., Hilliard, M., Lawrence, T., Trivedi, S., Colville-Nash, P., Bellingan, G., Fitzgerald, D., Yaqoob, M. M., and Gilroy, D. W. (2007) Hematopoietic prostaglandin D2 synthase controls the onset and resolution of acute inflammation through PGD2 and 15-deoxyDelta12 14 PGJ2. *Proc Natl Acad Sci U S A* **104**, 20979-20984
83. Gilroy, D. W., Colville-Nash, P. R., Willis, D., Chivers, J., Paul-Clark, M. J., and Willoughby, D. A. (1999) Inducible cyclooxygenase may have anti-inflammatory properties. *Nat Med* **5**, 698-701
84. Li, Z., Yang, G., Khan, M., Stone, D., Woo, S. L., and Wang, J. H. (2004) Inflammatory response of human tendon fibroblasts to cyclic mechanical stretching. *Am J Sports Med* **32**, 435-440
85. Werner, M., Jordan, P. M., Romp, E., Czapka, A., Rao, Z., Kretzer, C., Koeberle, A., Garscha, U., Pace, S., Claesson, H. E., Serhan, C. N., Werz, O., and Gerstmeier, J. (2019) Targeting biosynthetic networks of the proinflammatory and proresolving lipid metabolome. *FASEB J* **33**, 6140-6153
86. Serhan, C. N., Hamberg, M., Samuelsson, B., Morris, J., and Wishka, D. G. (1986) On the stereochemistry and biosynthesis of lipoxin B. *Proc Natl Acad Sci U S A* **83**, 1983-1987
87. Serhan, C. N., Nicolaou, K. C., Webber, S. E., Veale, C. A., Dahlen, S. E., Puustinen, T. J., and Samuelsson, B. (1986) Lipoxin A. Stereochemistry and biosynthesis. *J Biol Chem* **261**, 16340-16345
88. Hong, S., Gronert, K., Devchand, P. R., Moussignac, R. L., and Serhan, C. N. (2003) Novel docosatrienes and 17S-resolvins generated from docosahexaenoic acid in murine brain, human blood, and glial cells. Autacoids in anti-inflammation. *J Biol Chem* **278**, 14677-14687
89. Wang, Y., He, G., Tang, H., Shi, Y., Kang, X., Lyu, J., Zhu, M., Zhou, M., Yang, M., Mu, M., Chen, W., Zhou, B., Zhang, J., and Tang, K. (2019) Aspirin inhibits inflammation and scar formation in the injury tendon healing through regulating JNK/STAT-3 signalling pathway. *Cell Prolif* **52**, e12650
90. Lehner, C., Spitzer, G., Gehwolf, R., Wagner, A., Weissenbacher, N., Deininger, C., Emmanuel, K., Wichlas, F., Tempfer, H., and Traweger, A. (2019) Tenophages: a novel macrophage-like tendon cell population expressing CX3CL1 and CX3CR1. *Dis Model Mech* **12**
91. Gottfried, E., Kunz-Schughart, L. A., Weber, A., Rehli, M., Peuker, A., Muller, A., Kastenberger, M., Brockhoff, G., Andreesen, R., and Kreutz, M. (2008) Expression of CD68 in non-myeloid cell types. *Scand J Immunol* **67**, 453-463

- 926 92. Andersson, G., Backman, L. J., Scott, A., Lorentzon, R., Forsgren, S., and Danielson, P. (2011)  
 927 Substance P accelerates hypercellularity and angiogenesis in tendon tissue and enhances paratendinitis  
 928 in response to Achilles tendon overuse in a tendinopathy model. *Br J Sports Med* **45**, 1017-1022
- 929 93. Chbinou, N., and Frenette, J. (2004) Insulin-dependent diabetes impairs the inflammatory response and  
 930 delays angiogenesis following Achilles tendon injury. *Am J Physiol Regul Integr Comp Physiol* **286**,  
 931 R952-957
- 932 94. Fenwick, S. A., Hazleman, B. L., and Riley, G. P. (2002) The vasculature and its role in the damaged  
 933 and healing tendon. *Arthritis Res* **4**, 252-260
- 934 95. Nieman, D. C., Gillitt, N. D., Chen, G. Y., Zhang, Q., Sakaguchi, C. A., and Stephan, E. H. (2019)  
 935 Carbohydrate intake attenuates post-exercise plasma levels of cytochrome P450-generated oxylipins.  
 936 *PLoS One* **14**, e0213676
- 937 96. Nieman, D. C., Gillitt, N. D., Chen, G. Y., Zhang, Q., Sha, W., Kay, C. D., Chandra, P., Kay, K. L., and  
 938 Lila, M. A. (2020) Blueberry and/or Banana Consumption Mitigate Arachidonic, Cytochrome P450  
 939 Oxylipin Generation During Recovery From 75-Km Cycling: A Randomized Trial. *Front Nutr* **7**, 121
- 940 97. Signini, E. F., Nieman, D. C., Silva, C. D., Sakaguchi, C. A., and Catai, A. M. (2020) Oxylipin  
 941 Response to Acute and Chronic Exercise: A Systematic Review. *Metabolites* **10**
- 942 98. Trappe, T. A., Carroll, C. C., Jemiolo, B., Trappe, S. W., Dossing, S., Kjaer, M., and Magnusson, S. P.  
 943 (2008) Cyclooxygenase mRNA expression in human patellar tendon at rest and after exercise. *Am J*  
 944 *Physiol Regul Integr Comp Physiol* **294**, R192-199
- 945 99. McLennan, I. S., and Macdonald, R. E. (1991) Prostaglandin synthetase and prostacyclin synthetase in  
 946 mature rat skeletal muscles: immunohistochemical localisation to arterioles, tendons and connective  
 947 tissues. *J Anat* **178**, 243-253
- 948 100. Stanford, K. I., Lynes, M. D., Takahashi, H., Baer, L. A., Arts, P. J., May, F. J., Lehnig, A. C.,  
 949 Middelbeek, R. J. W., Richard, J. J., So, K., Chen, E. Y., Gao, F., Narain, N. R., Distefano, G., Shettigar,  
 950 V. K., Hirshman, M. F., Ziolo, M. T., Kiebish, M. A., Tseng, Y. H., Coen, P. M., and Goodyear, L. J.  
 951 (2018) 12,13-diHOME: An Exercise-Induced Lipokine that Increases Skeletal Muscle Fatty Acid  
 952 Uptake. *Cell Metab* **27**, 1111-1120 e1113
- 953 101. Christensen, B., Dandanell, S., Kjaer, M., and Langberg, H. (2011) Effect of anti-inflammatory  
 954 medication on the running-induced rise in patella tendon collagen synthesis in humans. *J Appl Physiol*  
 955 (1985) **110**, 137-141
- 956 102. Marsolais, D., Cote, C. H., and Frenette, J. (2003) Nonsteroidal anti-inflammatory drug reduces  
 957 neutrophil and macrophage accumulation but does not improve tendon regeneration. *Lab Invest* **83**, 991-  
 958 999

- 959 103. Plein, L. M., and Rittner, H. L. (2018) Opioids and the immune system - friend or foe. *Br J Pharmacol*  
960 **175**, 2717-2725

961  
962  
963  
964  
965  
966  
967  
968  
969  
970  
971  
972  
973  
974 **Figure Legends:**

975 **Figure 1. Divergent lipid mediator profiles of functionally related musculoskeletal tissues. A:** Complete  
976 metabolipidomic profile of lipid mediators detected by tandem liquid chromatography-mass spectrometry (LC-  
977 MS/MS) analysis of plantaris tendon homogenates from ambulatory control rats undergoing habitual cage  
978 activity ranked by absolute concentration normalized to tissue mass (pg/mg). **B:** Unsupervised principle  
979 component analysis (PCA) score plots of the overall LC-MS/MS profile of functionally associated plantaris  
980 tendon and muscle samples from ambulatory control rats. **C:** PCA loading plot showing the relative  
981 contributions of some representative analytes from each major enzymatic biosynthetic pathway to the  
982 musculotendinous mediator lipidomes. **D:** Percentage composition by biosynthetic pathway of the overall  
983 mediator lipidome of ambulatory plantaris muscle samples. **E:** Percentage composition by biosynthetic pathway  
984 of the overall mediator lipidome of ambulatory plantaris tendon samples. **D-E:** Linoleic acid (18:2n-6)  
985 metabolites (e.g. HODEs & EpOMEs) are excluded from graphical presentation and are shown separately in



Supplemental Table 1. **F:** Volcano plot showing the direction, magnitude, and statistical significance of lipid mediator concentrations between tendon and muscle. Each dot represents a single analyte, positive  $\text{Log}_2$  fold changes (FC) indicate lipid mediator concentrations which were enriched in tendon, and negative  $\text{Log}_2$  FC indicate those enriched in muscle. Analytes with +1.5 absolute FC (+0.58  $\text{Log}_2$  FC) or -1.5 FC (-0.58  $\text{Log}_2$  FC) between tissue type and unadjusted  $p < 0.05$  were considered to differ significantly between tendon and muscle samples. P-values were determined by two-tailed paired t-tests.

**Figure 2. Dynamic changes in lipid mediators in response to tendon overuse.** Changes in intratendinous concentrations of each individually detected lipid mediator species in overloaded plantaris tendons when compared to plantaris tendons obtained from ambulatory control rats at (A) day 3, (B) day 7, and (C) day 28 of recovery from synergist ablation-induced plantaris tendon overuse. Complete volcano plot source data is shown in Supplemental Table 3. **D:** Time-course changes in lipid mediator concentrations pooled over biosynthetic pathway in the overloaded plantaris tendon over the time-course of recovery from synergist ablation surgery. **E:** Time-course changes in intratendinous concentrations of a selection of major representative individual lipid mediator species from each biosynthetic pathway in response to tendon overuse. The data for the full panel of analytes monitored by the LC-MS/MS assay is shown in Supplemental Table 1. **F:** Changes in the relative contribution of major biosynthetic pathways to the overall tendon mediator lipidome following synergist ablation induced-tendon overuse. **D-F:** Linoleic acid (18:2n-6) metabolites (e.g. HODEs & EpOMEs) are excluded from graphical presentation and are shown in Supplemental Table 1. P-values were determined by two-tailed unpaired t-tests (panel A-C) or one-way ANOVA followed by Holm-Šidák post hoc tests (panel D).

014  
015  
016  
017  
018  
019 **Figure 3. Intramuscular infiltration of inflammatory cells in response to synergist ablation. A:** Overloaded  
020 plantaris muscles were collected from Sprague Dawley rats at day 3, 7, and 28 following synergist ablation  
021 surgery. Plantaris muscles from ambulatory age and sex matched rats served as non-surgical controls. Tissue  
022 cross-sections were cut from the plantaris muscle midbelly and stained with antibodies against  
023 polymorphonuclear cells (PMNs, HIS48<sup>+</sup>), inflammatory ED1 monocytes/macrophages (MΦ, CD68<sup>+</sup>), and  
024 resident/M2-like ED2 MΦ (CD163<sup>+</sup>). Scale bars are 50 μm. Additional examples of representative images and  
025 quantitative analysis are presented in References no. 48.

026  
027  
028  
029  
030  
031  
032  
033  
034  
035  
036  
037  
038

039  
040 **Figure 4. Peritendinous infiltration of inflammatory cells in response to synergist ablation-induced**  
041 **tendon overuse. A:** Overloaded plantaris tendons were collected from Sprague Dawley rats at day 3, 7, and 28  
042 following synergist ablation surgery. Plantaris tendons from ambulatory age and sex matched rats served as  
043 non-surgical controls. Tissue cross-sections were cut from the tendon mid-substance and stained with antibodies  
044 against polymorphonuclear cells (PMNs, HIS48<sup>+</sup>), inflammatory ED1 monocytes/macrophages (MΦ, CD68<sup>+</sup>),  
045 and resident/M2-like ED2 MΦ (CD163<sup>+</sup>). Images were captured from the periphery of control plantaris tendons  
046 (epitenon region), or from within the center of the expanded peritendinous tissue layer at the periphery of  
047 overloaded plantaris tendons (neotendon matrix). Scale bars are 50 μm. Quantification of peritendinous  
048 infiltration of **(B)** PMNs (HIS48<sup>+</sup> cells), **(C)** ED1 MΦ (CD68<sup>+</sup> cells), **(D)** ED2 MΦ (CD163<sup>+</sup> cells), and **(E)**  
049 Total myeloid cells (sum of PMNs, ED1 MΦ and ED2 MΦ). Values are mean ± SEM of 5-7 plantaris tendon  
050 per time-point with dots representing data from each individual tendon. P-values were determined by one-way  
051 ANOVA followed by Holm-Šidák post hoc tests.

052  
053  
054  
055  
056  
057  
058  
059  
060  
061  
062 **Figure 5. Inflammatory macrophage infiltration of the original tendon core following plantaris overuse.**  
063 **A:** Overloaded plantaris tendons were collected from Sprague Dawley rats at day 3, 7, and 28 following  
064 synergist ablation-induced tendon overuse. Plantaris tendons from ambulatory age and sex matched rats served  
065 as non-surgical controls. Tissue cross-sections were cut from the tendon mid-substance and stained with  
066 antibodies against polymorphonuclear cells (PMNs, HIS48<sup>+</sup> cells), inflammatory ED1 monocytes/macrophages

(MΦ, CD68<sup>+</sup> cells), and resident/M2-like ED2 MΦ (CD163<sup>+</sup> cells). Representative images were captured from the center of the dense original tendon core (control, day 7, and day 28), or at the junction of the tendon core and the epitenon/immature neotendon (day 3). Scale bars are 50 μm.

**Figure 6: Local expression of inflammation-related genes in response to synergist ablation-induced plantaris tendon overuse.** Overloaded plantaris tendons were collected from male Sprague Dawley rats at day 3, 7, and 28 following synergist ablation surgery. Plantaris tendons from ambulatory age and sex matched rats served as non-surgical controls. Total tendon RNA was extracted, reverse transcribed to cDNA, and expression of inflammation-related genes measured by real-time quantitative reverse transcription PCR (RT-qPCR). Relative mRNA expression (fold change from control) was determined for (A) CD11b (*Itgam*), (B) CD68 (*Cd68*), (C) EMR1 (rat analog of F4/80, *Adgre1*), (D) CD163 (*Cd163*), (E) CD206 (*Mrc1*), (F) cyclooxygenase-1 (COX-1, *Ptgs1*), and (G) cyclooxygenase-2 (COX-2, *Ptgs2*). Beta-2-Microglobulin (*B2m*) served as an endogenous control for normalization of genes of interest. Bars show the mean ± SEM of 8-12 plantaris tendons from 4-6 rats per group with dots representing data from each individual tendon sample. P-values were determined by one-way ANOVA followed by Holm-Šidák post hoc tests.

**Table 1:** Real-time reverse transcription PCR primers

<b>Gene</b>		<b>Sequence</b>
<i>Ilgam</i>	F	TGTACCACTCATTGTGGGCA
	R	AGCCAAGCTTGTATAGGCCAG
<i>Cd68</i>	F	TCCAGCAATTCACCTGGACC
	R	AAGAGAAGCATGGCCCGAAG
<i>Adgre1</i>	F	CTTCTGGGGAGCTTACAATGG
	R	TGTGGTTCTGAACTGCACGA
<i>Cd163</i>	F	CTGAAATCCTCGGGTTGGCA
	R	TGTAGCTGTGGTCATCCGTG
<i>Mrc1</i>	F	TCAACTCTTGGACTCACGGC
	R	ATGATCTGCGACTCCGACAC
<i>Ptgs1</i>	F	AGTACCAGGTGCTGGATGGAGA
	R	GGAGCAACCCAAACACCTCC
<i>Ptgs2</i>	F	ACGTGTTGACGTCCAGATCA
	R	GGCCCTGGTGTAGTAGGAGA
<i>B2m</i>	F	CACTGAATTCACACCCACCG

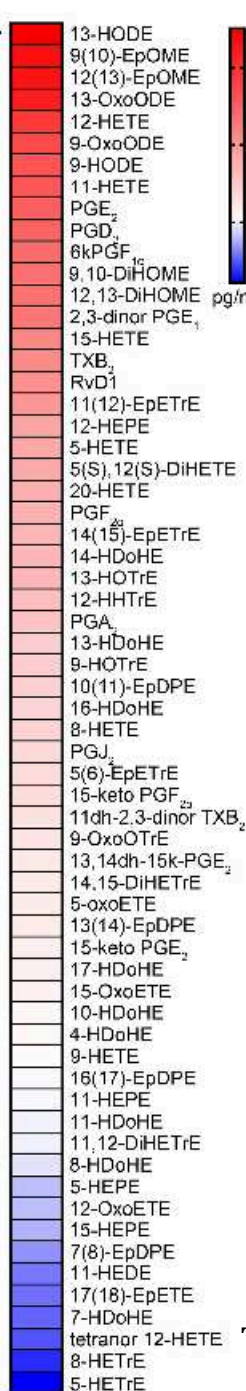
**Table 2:** Changes in tendon mass and RNA content in response to overuse

	Control	Day 3	Day 7	Day 28	
Tendon mass (mg)	14.76 ± 1.23	13.36 ± 2.09	25.95 ± 6.89	32.60 ± 7.70	*
RNA concentration (ng/mg)	65.91 ± 7.80	239.38 ± 17.48 ***	165.81 ± 19.84 ***	105.21 ± 11.67	
Total RNA content (µg)	0.94 ± 0.11	3.26 ± 0.55 **	3.74 ± 0.75 ***	3.31 ± 0.70 **	

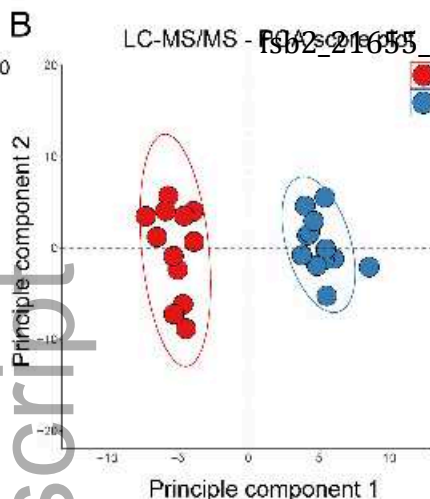
Values are mean ± SEM of 8-12 plantaris tendons from 4-6 rats/group. \*p<0.05, \*\*p<0.01, \*\*\*p<0.001 vs. control

Author Manuscript

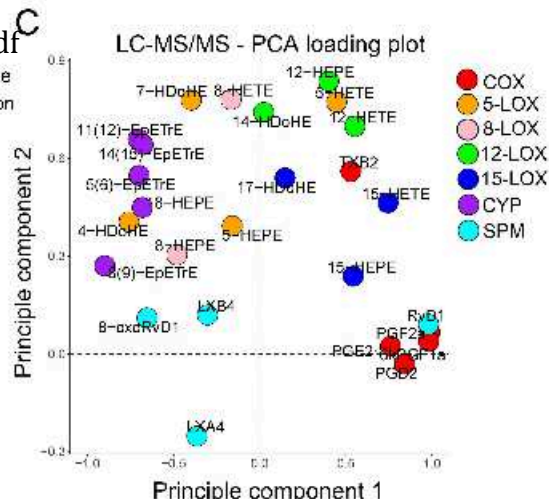
A



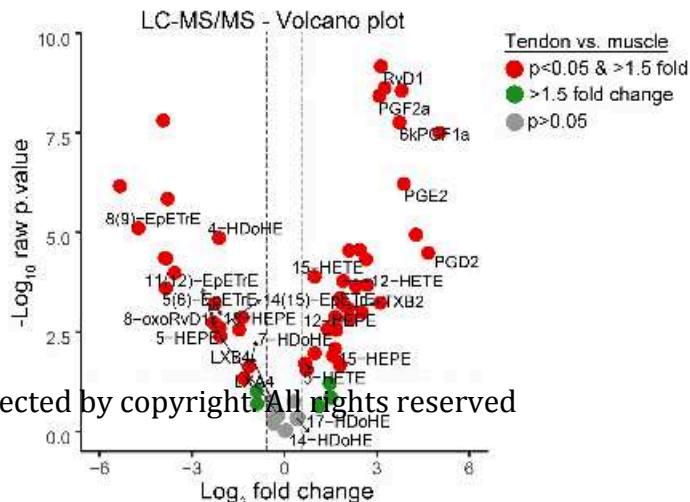
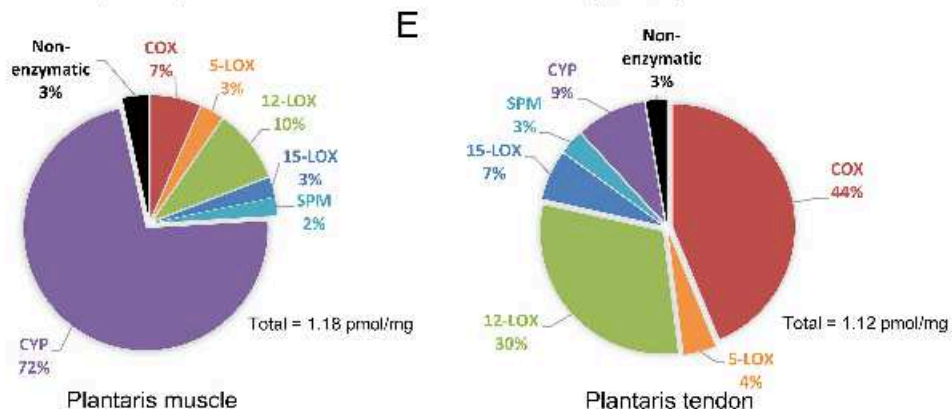
B



C

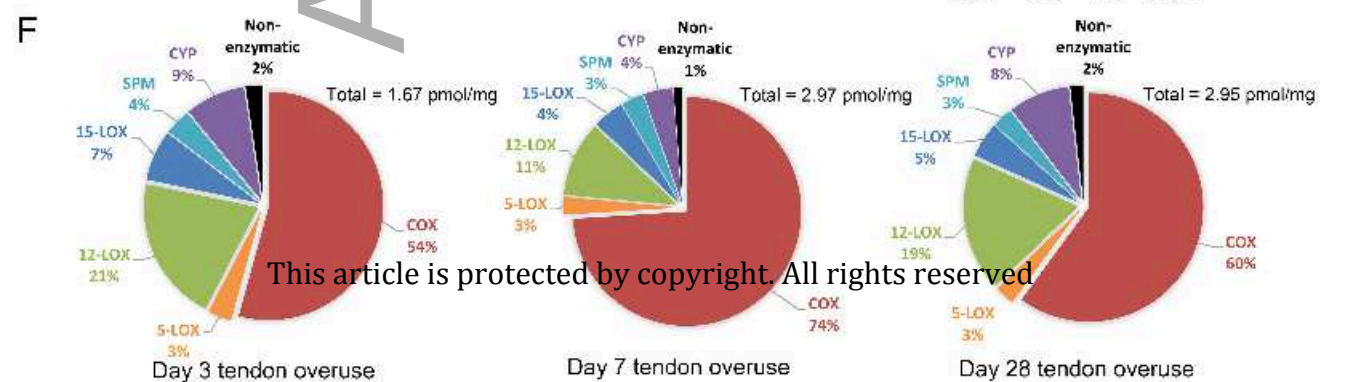
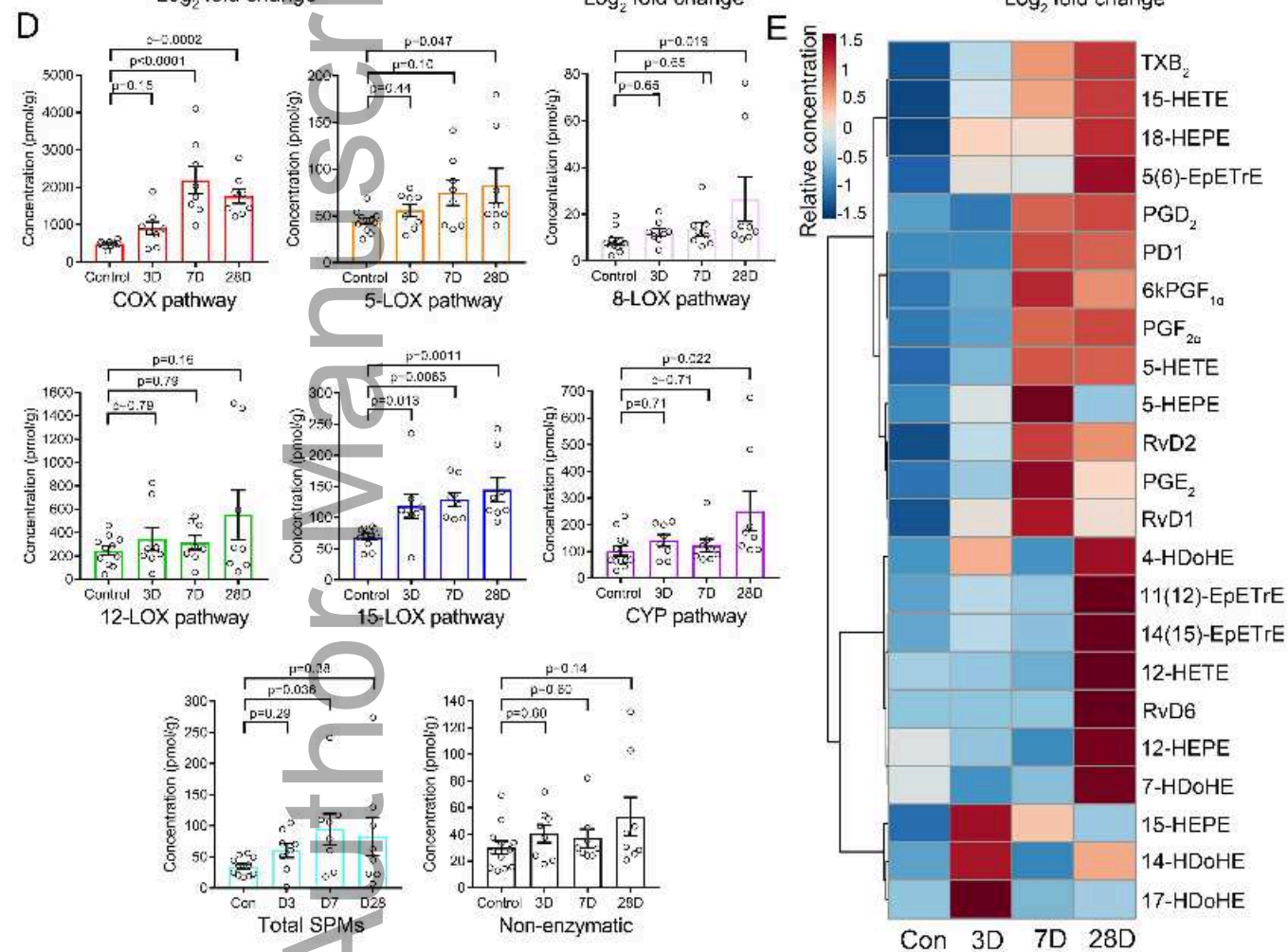
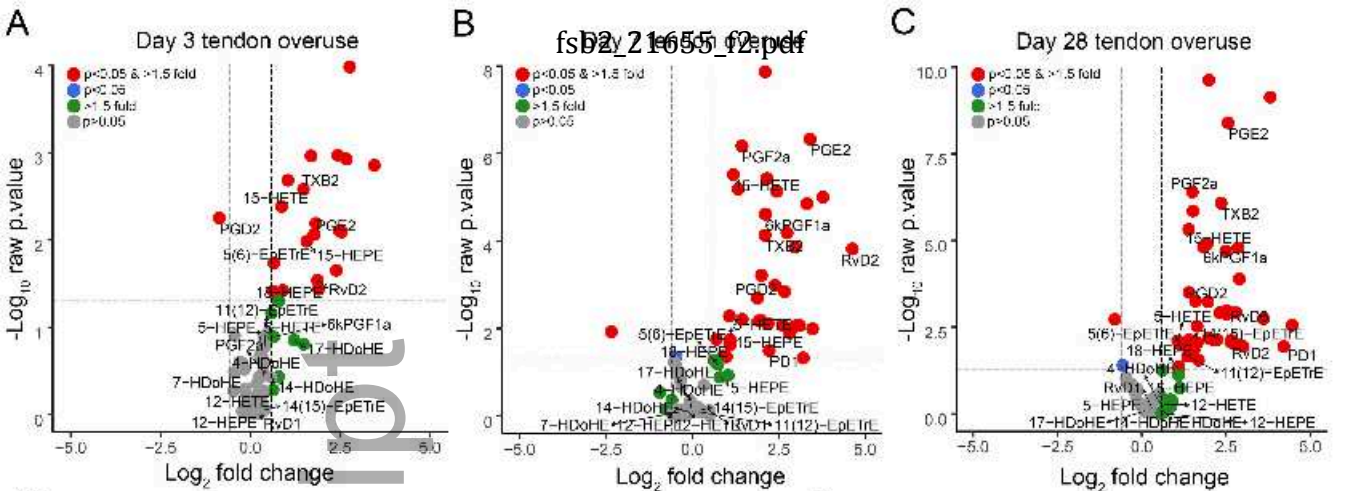


E



This article is protected by copyright. All rights reserved

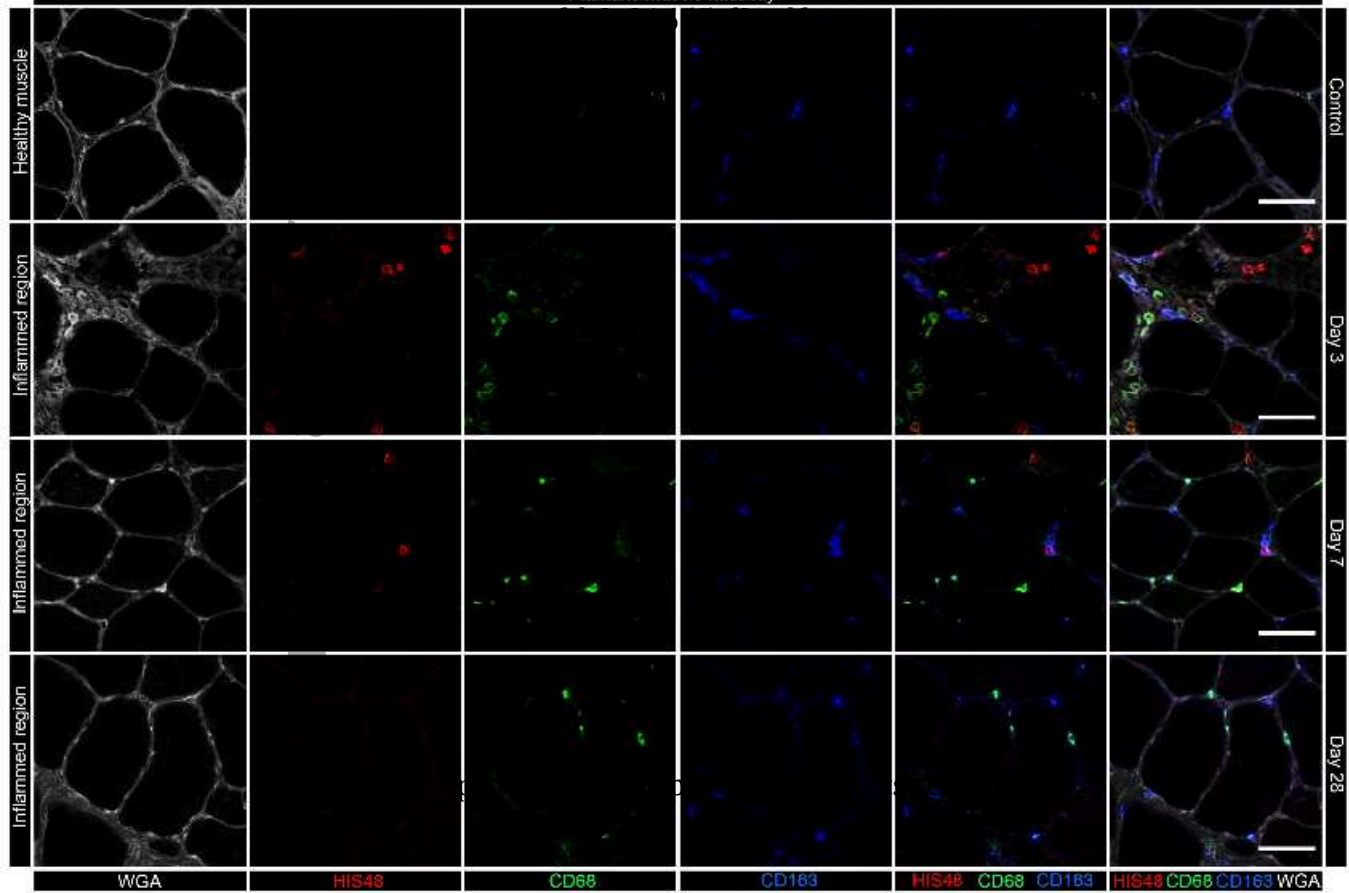
Author Manuscript

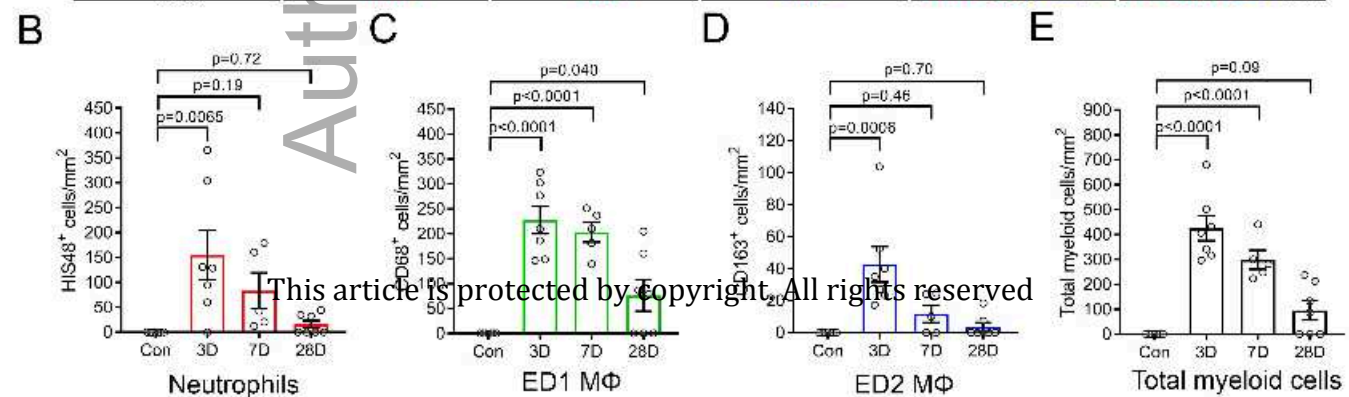
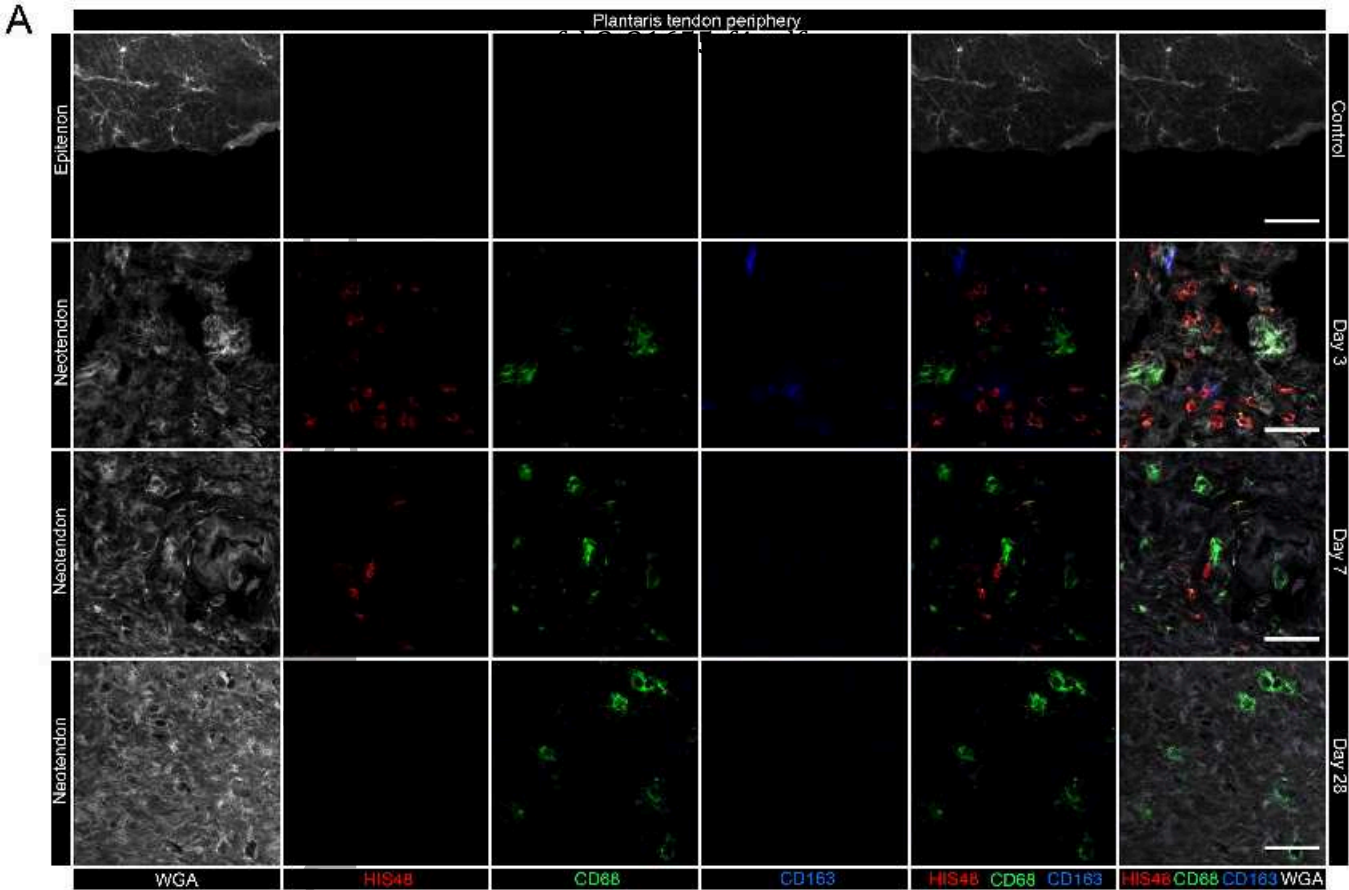


This article is protected by copyright. All rights reserved

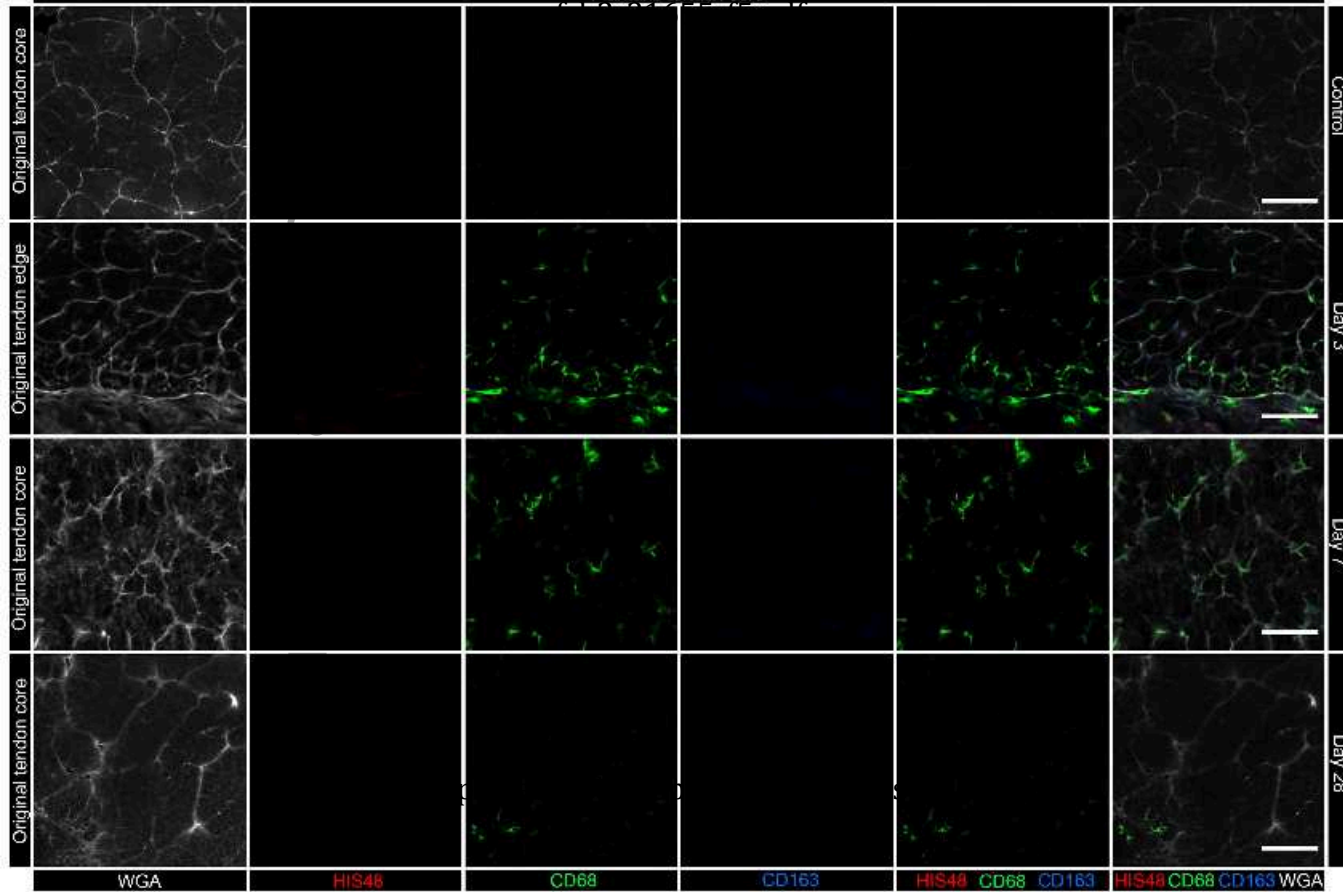


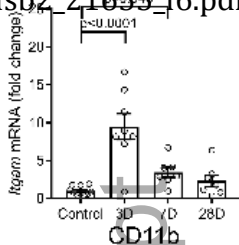
## Plantaris muscle midbelly



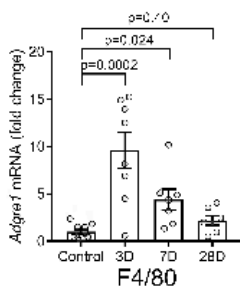
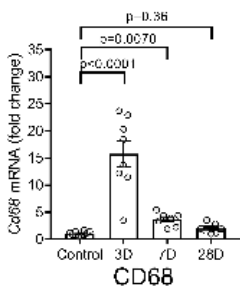


## Plantaris tendon core

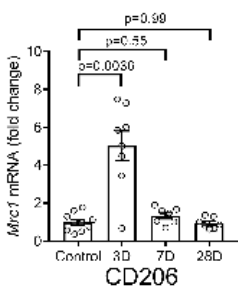
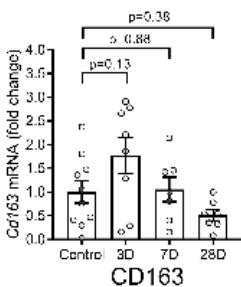




B



D



F

